"There is nothing more practical than a good theory."

– Vladimir Vapnik

University of Alberta

DECONVOLUTION FILTER DESIGN WITH GUARANTEED ENERGY-TO-PEAK
PERFORMANCE

by

Jing Zhou ©

A thesis submitted to the Faculty of Graduate Studies and Research in partial
fulfillment of the requirements for the degree of **Master of Science.**

Department of Electrical and Computer Engineering

Edmonton, Alberta
Fall 2008

Canada

To my husband and my son

Abstract

Deconvolution filtering problems in dynamic systems have wide applications in seismology, oil exploration, image restoration, fault detection, signal processing, communications, and equalization. This thesis aims at designing deconvolution filters with guaranteed energy-to-peak performance.

In Chapter 2, we consider the design of $l_2 - l_\infty$ deconvolution filters. We first formulate the FIR deconvolution filtering problem, and then derive the sufficient and necessary condition to satisfy the design objectives. Further, the condition is transformed to LMIs with nonconvex constraints, which can be efficiently solved by the product reduction algorithm (PRA).

In Chapter 3, we study the $l_2 - l_\infty$ IIR deconvolution filter design. The sufficient and necessary condition is derived to guarantee the $l_2 - l_\infty$ filtering performance. Further, the condition is transformed to LMIs.

In practice, the channel uncertainty is an important factor to consider. Therefore in Chapter 4, to incorporate the channel uncertainties, we propose to use the polytopic uncertainty description, and derive the sufficient condition to guarantee the robust $l_2 - l_\infty$ IIR deconvolution filtering performance. In order to further decrease the conservativeness of the design, we apply the parameter-dependent Lyapunov method and improve the robust $l_2 - l_\infty$ IIR deconvolution filter design.

Finally, several open problems are listed as the future research directions.

Acknowledgements

Contents

List of Figures

List of Tables

Chapter 1

Introduction

1.1 Deconvolution Filtering

The deconvolution filtering problem is to reconstruct a signal embedded in noise and distorted by the signal transmission channel. The deconvolution filtering problems in dynamic systems have wide applications in seismology, oil exploration, image restoration, fault detection, signal processing, communications, and equalization. As depicted in Figure 1.1, the perfect reconstruction (PR) is defined as the property wherein the reconstructed output signal is simply a delayed version of the input signal. However, due to the existence of model uncertainties and disturbances, it is hard to achieve PR. Therefore, a practical design objective is to reconstruct the signal S at the receiver end as close as possible, i.e., $\hat{S} \to S$. From the model matching perspective, as shown in Figure 1.2, the objective is alternatively to force e to be as small as possible.

In the following, we will generally classify current research on the design of deconvolution filters into three categories based on their different performance measures.

1.2 Design of Deconvolution Filters

There are mainly three performance measures under which deconvolution filtering problems have been considered: (1) the $\mathcal{H}_2$ performance measure, (2) the $\mathcal{H}_\infty$ performance measure, and (3) the mixed $\mathcal{H}_2/\mathcal{H}_\infty$ performance measure. In what follows, different design methods for deconvolution filters in the literature are classified into three main categories and reviewed.
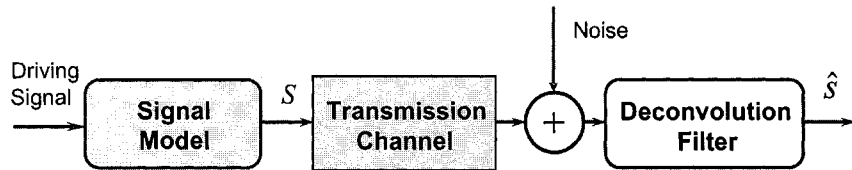
Figure 1.1: A general block-diagram of the deconvolution filtering system.
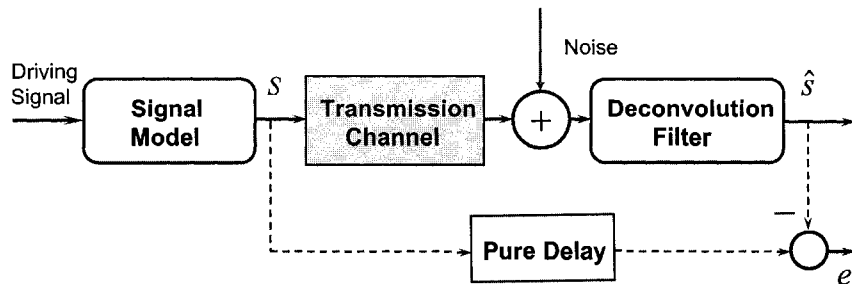
Figure 1.2: Model matching for a deconvolution filtering system.

1.2.1 $\mathcal{H}_2$ Deconvolution Filter Design

Chen, *et. al* studied the fixed-order infinite impulse response (IIR) and finite impulse response (FIR) $\mathcal{H}_2$ optimal deconvolution filter designs in [8]. How to optimally determine the coefficients of a fixed-order deconvolution filter to achieve the $\mathcal{H}_2$ minimization of reconstruction error is a highly nonlinear minimization problem, and thus, they proposed to apply the genetic algorithm to effectively solve the formulated nonlinear optimization problem.

In [12], the $\mathcal{H}_2$ optimal estimation of a linear combination of the state and the input of a discrete-time linear time-invariant dynamic system was investigated. Such a problem was reformulated in terms of three linear matrix inequalities (LMIs) and explicit formulae to compute a family of solutions for such LMIs were derived. This family is explicitly parameterized so that the $\mathcal{H}_2$ performance of the corresponding filter may be rendered arbitrarily close to the optimality by choosing certain involved parameters. It is worth mentioning that the formulation (of estimating a linear

combination of the state and the input) is pretty general and provides a unifying framework where several generalized versions of the $\mathcal{H}_2$ optimal estimation problem can be covered and solved, i.e., the state estimation, deconvolution, and input and state co-estimation.

In [66], the $\mathcal{H}_2$-optimal deconvolution problem for periodic FIR and IIR channels was studied. It showed that the 2-norm of a periodic filter can be directly quantified in terms of periodic system matrices and LMIs without resorting to the commonly used lifting technique. The optimal signal reconstruction problem was then formulated as an optimization problem subject to a set of matrix inequality constraints. Under this framework, the optimization of both the FIR and IIR periodic deconvolution filters can be made convex, solved using the interior point method, and computed by using the MATLAB LMI Toolbox. The robust deconvolution problem for periodic FIR and IIR channels with polytopic uncertainties were further solved, also by convex optimization and LMIs. Compared with the lifting approach to the design of periodic filters, the proposed approach is simpler yet more powerful in dealing with multi-objective deconvolution problems and channel uncertainties.

1.2.2 $\mathcal{H}_\infty$ Deconvolution Filter Design

Compared with conventional $\mathcal{H}_2$ deconvolution, the $\mathcal{H}_\infty$ deconvolution has some practical advantages. There is no need to know exactly the knowledge of statistics of the driving and measurement noises, and the noises are only needed to have bounded energy, thus the $\mathcal{H}_\infty$ deconvolution has more robustness to the noises than the $\mathcal{H}_2$ deconvolution.

In [8], genetic algorithms were also applied to deal with the $\mathcal{H}_\infty$ optimal signal reconstruction design problem with a prescribed filter order. Genetic algorithms are optimization and machine learning algorithms, initially inspired from the processes of natural selection and evolutionary genetics. They tend to achieve the global

optimum solution without becoming trapped at local minima. The convergence property of the proposed design algorithm was also analyzed.

In [28], the $\mathcal{H}_\infty$ deconvolution filtering for a linear time-varying discrete-time system was studied under the framework of Krein space [20]. The $\mathcal{H}_\infty$ deconvolution filter was designed in terms of solutions of Riccati equations. A sufficient and necessary condition for an $\mathcal{H}_\infty$ deconvolution filter was established.

A reduced-order $\mathcal{H}_\infty$ deconvolution filter design based on the bounded real lemma for linear discrete-time systems was proposed in [43]. The order of the proposed deconvolution filter is less than or equal to $n - p$, where n and p are orders of the system and the measurement, respectively. The filter parameters were expressed in closed form in terms of a solution to a Riccati difference equation.

In [55], the authors studied the robust $\mathcal{H}_\infty$ deconvolution filtering problem for continuous- and discrete-time stochastic systems with interval uncertainties. The matrices of the system describing the signal transmissions are assumed to be uncertain within given intervals, and the stochastic perturbation is in the form of a multiplicative Gaussian white noise with constant variance. Finally, the filter parameters were characterized in terms of the solution to LMIs.

Linear periodic systems and filters can find many applications in communications, filtering, decoding, network synthesis, process control, and so on. Xie *et. al* studied the deconvolution problem for linear periodic transmission channels subject to the $\mathcal{H}_\infty$ performance specification [58]. Further, Xie *et. al* investigated the $\mathcal{H}_\infty$ deconvolution problem for 2-D digital systems described by the Fornasini-Marchesini local state-space (FM LSS) model [57].

1.2.3 Mixed $\mathcal{H}_2/\mathcal{H}_\infty$ Deconvolution Filter Design

To enjoy the benefits of both $\mathcal{H}_2$ and $\mathcal{H}_\infty$ performance measures, the mixed $\mathcal{H}_2/\mathcal{H}_\infty$ optimal deconvolution filter design was proposed in [21]. Genetic algorithm was

introduced to treat the nonlinear optimization design problem of the fixed-order mixed $\mathcal{H}_2/\mathcal{H}_\infty$ deconvolution filter. Such a mixed design can achieve the $\mathcal{H}_2$ optimal reconstruction and a desired robustness against the effect of uncertainties from the $\mathcal{H}_\infty$ norm perspective.

1.3 Energy-to-Peak $(l_2 - l_\infty)$ Performance Measure

In this section, we introduce the energy-to-peak performance measure under the framework of filtering. The energy-to-peak performance measure is also referred to as the $l_2 - l_\infty$ one.

Let us start with briefly revisiting the popular Kalman filtering and $\mathcal{H}_\infty$ filtering problems. In general, the filtering problem is to estimate the states of a system using past measurements. The celebrated Kalman filter provides a recursive algorithm to minimize the variance of the state estimation error when the power spectral density of the process and the measurement noise is known [3]. Kalman filtering techniques have found widespread applications in aerospace guidance, navigation, and control problems. $\mathcal{H}_\infty$ filtering has received considerable attention recently. Unlike the traditional Kalman filtering, it does not require knowledge of the statistical properties of the noise. Its objective is to minimize the energy of the estimation error for the worst possible bounded energy disturbance.

The objective of the filtering design with guaranteed energy-to-peak performance, i.e., $l_2 - l_\infty$ filtering is to minimize the peak value of the estimation error for all possible bounded energy disturbances. Hence, the $l_2 - l_\infty$ filtering can be considered as a deterministic formulation of the Kalman filter [18].

For a discrete-time vector-valued signal $f(k)$, the l_2 norm is

$$\|f\|_2 = \left\{ \sum_0^\infty f^{\mathrm{T}}(k)f(k) \right\}^{1/2} ,$$

where $(\cdot)^{\mathrm{T}}$ denotes the transpose of a real matrix. The l_∞ norm is

$$\|f\|_\infty = \sup_k \left\{ f^{\mathrm{T}}(k) f(k) \right\}^{1/2}.$$

Consider a stable n-th order linear time-invariant system with a state-space representation

$$
\begin{aligned}
x(k+1) &= Ax(k) + Bw(k), \\
y(k) &= Cx(k) + Dw(k), \\
z(k) &= Lx(k).
\end{aligned}
$$

Here, A, B, C, D, and L are system matrices with appropriate dimensions, $x(k) \in \mathbb{R}^n$ is the state vector, $y(k) \in \mathbb{R}^p$ is the measured output, and $z(k) \in \mathbb{R}^r$ is the signal to be estimated.

The discrete-time $l_2 - l_\infty$ filtering problem is to find a filter $\mathcal{F}$ with state-space formulation and order $\hat{n} \leq n$ to minimize the peak value $\|e\|_\infty$ of the estimation error $e(k) = z(k) - \hat{z}(k)$ over all bounded energy disturbances $w(k)$, that is

$$\min_{\mathcal{F}} \sup_{0 \neq w \in l_2} \frac{\|e\|_\infty}{\|w\|_2}.$$

1.4 Relationship of the $L_2 - L_\infty$ Induced Norm and $\mathcal{H}_2$ Norm

It is interesting and useful to revisit and clarify the relationship between the $L_2 - L_\infty$ induced norm and the $\mathcal{H}_2$ norm. This section is summarized and presented for continuous-time systems based on the following papers and the references therein: [56, 11, 44, 18].

For a finite-dimensional linear time-invariant feedback system, suppose $\mathcal{G}$ denotes the plant and $\mathcal{C}$ the controller; the signal w denotes the exogenous input vector, while z denotes the controller output vector; the signals u and y represent the control

input vector and the measured output vector, respectively. Let $\mathcal{T}_{zw}$ stand for the closed-loop map from the exogenous input w to the controlled output z.

Wilson [56] introduced several useful "system gains". Assume that the above-mentioned feedback system is internally stable, and T_{zw} denote the closed-loop transfer matrix from w to z. In [56], Wilson pointed out that, if T_{zw} is strictly proper, $\mathcal{T}_{zw}$ is a bounded operator from $L_2[0, \infty)$ to $L_\infty[0, \infty)$, and its induced norm is given by

$$\|\mathcal{T}_{zw}\| = \sqrt{f\left(\frac{1}{2\pi}\int_{-\infty}^{\infty} T_{zw}(j\omega)T_{zw}^*(j\omega)d\omega\right)}. \tag{1.1}$$

The function $f(\cdot)$ is either the maximum eigenvalue or the maximum diagonal entry.

First, when z is a scalar signal, (1.1) reduces to the $\mathcal{H}_2$ norm of T_{zw}. Second, if z is a vector-valued signal, then this induced norm is no longer the standard $\mathcal{H}_2$ norm.

1.5 Motivation and Objectives

The work of the thesis is motivated by the following observations based on a comprehensive literature review:

1. In the literature, there was no reported work on the $l_2 - l_\infty$ deconvolution filter design, to the best of author's knowledge.

2. In practice, channel uncertainty is an important factor to consider. However, in the area of deconvolution filter design, this issue has received relatively less attention.

Therefore, the main objectives of this thesis lie in the following aspects:

1. To develop $l_2 - l_\infty$ deconvolution filter design methods, for both finite impulse response (FIR) and infinite impulse response (IIR) structures.

2. To design ease-to-solve algorithms based on the LMI techniques.

3. To incorporate the channel polytopic uncertainties into the robust IIR deconvolution filter design.

To proceed, it is worthwhile summarizing different filters in the following table. According to specific application requirements, different types of filter design methods should be chosen.

Table 1.1: Filters with different performance measures

Filter	Performance	Mathematic Description
Kalman	Mean Squared Error	$\min(E\|e\|_2^2)$
$\mathcal{H}_2$	Least Squared Error	$\min(\|e\|_2^2)$
$\mathcal{H}_\infty$	Maximal Energy Gain	$\|G_{e\omega}\|_\infty^2 < \gamma^2$ or $\sup \frac{\|e\|_2}{\|\omega\|_2} < \gamma$
$l_2 - l_\infty$	Maximal Energy-to-peak Gain	$\sup \frac{\|e\|_\infty}{\|\omega\|_2} < \gamma$

1.6 Scope of the Thesis

In Chapter 2, we consider the design of $l_2 - l_\infty$ deconvolution filters. We first formulate the FIR deconvolution filtering problem, and then derive the sufficient and necessary condition to satisfy the design objectives. Further, the condition is transformed to LMIs with nonconvex constraints, which can be efficiently solved by the product reduction algorithm (PRA).

In Chapter 3, we study the $l_2 - l_\infty$ IIR deconvolution filter design. The sufficient and necessary condition is derived to guarantee the $l_2 - l_\infty$ filtering performance. Further, the condition is transformed to LMIs.

In practice, the channel uncertainty is an important factor to consider. Therefore in Chapter 4, to incorporate the channel uncertainties, we propose to use the polytopic uncertainty description, and derive the sufficient condition to guarantee the robust $l_2 - l_\infty$ IIR deconvolution filtering performance. In order to further decrease

the conservativeness of the design, we apply the parameter-dependent Lyapunov function method and improve the robust $l_2 - l_\infty$ IIR deconvolution design.

The last chapter summarizes the work in the thesis, and outlines some possible future research directions.

1.7 Notation

The notation used throughout the thesis is fairly standard. The superscript 'T' stands for matrix transposition; $\mathbb{R}^n$ denotes the n-dimensional Euclidean space; $\mathbb{R}^{m \times n}$ is the set of all $m \times n$ real matrices; and the notation $P > 0$ means that P is symmetric and positive definite. In addition, in symmetric block matrices or long matrix expressions, we use $*$ as an ellipsis for the terms that are represented by symmetry and diag$\{\cdots\}$ represents a block-diagonal matrix.

Chapter 2

FIR Deconvolution Filter Design with Guaranteed Energy-to-Peak Performance

2.1 Introduction

In recent years, problems of the finite impulse response (FIR) deconvolution filter design for discrete-time channels have received considerable attention. In [48], the FIR deconvolution filter was designed such that the $\mathcal{H}_\infty$ norm of the filtering error transfer function is minimized subject to the constraint that the filter output with a given input to the system is constrained or bounded in a prescribed envelope. The filter design problem was further formulated as a standard optimization problem with LMI constraints. Further in [25], the channel uncertainties characterized by the integral quadratic constraints were incorporated to design the robust FIR deconvolution filters.

Other methods for discrete-time systems with partially known noise information are l_1 filtering and $l_2 - l_\infty$ filtering, which receive relatively less attention compared with $\mathcal{H}_\infty$ filtering. To the best of our knowledge, $l_2 - l_\infty$ filtering has not been applied to deconvolution filter design in the literature.

On the other hand, LMIs have gained much attention for their computational tractability and usefulness in control engineering. The number of control and estimation problems that can be formulated as LMI problems is large and continues to grow. LMIs can now be solved efficiently using the powerful MATLAB LMI Toolbox.

This chapter is concerned with the $l_2 - l_\infty$ FIR deconvolution filter design problem. The objective is to design deconvolution FIR filters by minimizing the peak value of the estimation error for all possible bounded energy disturbances.

The rest of this chapter is organized in the following way. We first formulate the FIR filtering problem and state the objective of $l_2 - l_\infty$ filtering design in Section 2.2. In Section 2.3, the sufficient and necessary condition is derived to guarantee the $l_2 - l_\infty$ filtering performance. Further, the condition is transformed to LMIs with

nonconvex constraints, which can be efficiently solved by the product reduction algorithm (PRA) [33, 63]. To illustrate the effectiveness of the proposed method, design examples are given in Section 2.4. Finally, the conclusion remarks are addressed in Section 2.5.

2.2   Problem Formulation

Consider the deconvolution filtering system shown in Figure 2.1. In the system, the source signal $s(k) \in \mathcal{R}$ is assumed to be generated by the signal model

Figure 2.1: An FIR deconvolution filtering system model.

$$\sum S : \left\{ \begin{array}{rcl} x_s(k+1) & = & A_s x_s(k) + B_s w(k) \\ s(k) & = & C_s x_s(k) + D_s w(k) \end{array} \right. , \qquad (2.1)$$

where $x_s(k) \in \mathbb{R}^{n_s}$ is the model state vector, $w(k) \in l_2[0, \infty)$ is the driving signal of the model, and A_s, B_s, C_s, and D_s are known constant matrices of appropriate dimensions. The source signal is transmitted through a channel modeled by

$$\sum C : \left\{ \begin{array}{rcl} x_c(k+1) & = & A_c x_c(k) + B_c s(k) \\ z_c(k) & = & C_c x_c(k) + D_c s(k), \end{array} \right. , \qquad (2.2)$$

where $x_c(k) \in \mathbb{R}^{n_c}$ is the channel state vector.

At the receiver end, the measured signal $y(k)$ is equal to $z_c(k) + v(k)$, where $v(k)$ is the energy-bounded channel noise. To optimally recover the source signal $s(k)$, the signal $y(k)$ is deconvoluted by an FIR filter of length n_f with the transfer

function

$$F(z) = a_0 + a_1 z^{-1} + a_2 z^{-2} + \cdots + a_{n_f} z^{-n_f},$$

where a_0, a_1, $\cdots$, a_{n_f} are filter parameters to be designed, and n_f is the order of the FIR filter. The FIR filter can also be represented by the following state-space model

$$\sum F : \left\{ \begin{array}{rcl} x_f(k+1) & = & A_f x_f(k) + B_f y(k) \\ \hat{s}(k) & = & C_f x_f(k) + D_f y(k) \end{array} \right. , \qquad (2.3)$$

where $x_f(k) \in \mathbb{R}^{n_f}$ is the filter state vector, and A_f, B_f, C_f, and D_f are constant matrices to be designed, and they have the following form:

$$A_f = \begin{bmatrix} 0 & 1 & 0 & \cdots & 0 \\ 0 & 0 & 1 & \cdots & 0 \\ \vdots & \vdots & \vdots & & \vdots \\ 0 & 0 & 0 & \cdots & 1 \\ 0 & 0 & 0 & \cdots & 0 \end{bmatrix}_{n_f \times n_f},$$

$$B_f = \begin{bmatrix} 0 \\ 0 \\ \vdots \\ 0 \\ 1 \end{bmatrix}_{n_f \times 1},$$

$$C_f = \begin{bmatrix} a_{n_f} & a_{n_f-1} & \cdots & a_1 \end{bmatrix}_{1 \times n_f},$$

$$D_f = a_0.$$

Define the filtering error as

$$e(k) = s(k) - \hat{s}(k).$$

Then the filtering error system can be described as

$$\sum e : \left\{ \begin{array}{rcl} x_e(k+1) & = & A_e x_e(k) + B_e w_e(k) \\ e(k) & = & C_e x_e(k) + D_e w_e(k) \end{array} \right. , \qquad (2.4)$$

where $x_e^T(k) = \begin{bmatrix} x_s^T(k), & x_c^T(k), & x_f^T(k) \end{bmatrix}$, $w_e^T(k) = \begin{bmatrix} w^T(k), & v^T(k) \end{bmatrix}$, and

$$A_e = \begin{bmatrix} A_s & 0 & 0 \\ B_c C_s & A_c & 0 \\ B_f D_c C_s & B_f C_c & A_f \end{bmatrix},$$

14

$$B_e = \begin{bmatrix} B_s & 0 \\ B_c D_s & 0 \\ B_f D_c D_s & B_f \end{bmatrix},$$

$$C_e = \begin{bmatrix} C_s - D_f D_c C_s & -D_f C_c & -C_f \end{bmatrix},$$

$$D_e = \begin{bmatrix} D_s - D_f D_c D_s & -D_f \end{bmatrix}.$$

The main objective of this work is to develop the $l_2 - l_\infty$ FIR filter of the form in (2.3) such that:

1. The filtering error system is stable.

2. The filtering error system guarantees

$$\|e\|_\infty \leqslant \gamma \|w_e\|_2$$

for all nonzero $w_e \in l_2[0, \infty)$, where $\|w_e\|_2^2 := \sum_{k=0}^\infty w_e^T(k) w_e(k)$, $\|e\|_\infty^2 = \sup_k e^T(k) e(k)$, and $\gamma > 0$ is a pre-selected scalar.

2.3 FIR $l_2 - l_\infty$ Filter Design

In this section, we solve the FIR $l_2 - l_\infty$ deconvolution filter design problem under the framework of LMIs. The sufficient and necessary condition is first derived and further converted to equivalent LMIs with nonconvex constraints.

First of all, we state the following lemma that is adapted from Lemma 7 in [18].

Lemma 1 *Suppose (A_e, B_e, C_e, D_e) is arbitrary but fixed and let $\gamma > 0$ be given. Then the filtering error system is stable and the $l_2 - l_\infty$ gain of the filtering error system is less than γ, that is*

$$\sup_{0 \neq w \in l_2} \frac{\|e\|_\infty}{\|w\|_2} < \gamma, \tag{2.5}$$

if and only if there exists a matrix $P > 0$ such that

$$C_e P C_e^T + D_e D_e^T < \gamma^2 I, \tag{2.6}$$

15

$$A_e P A_e^{\mathrm{T}} - P + B_e B_e^{\mathrm{T}} < 0. \tag{2.7}$$

Proof: It can be proved by following the results in [18, 16]. $\square$

Then we have the following theorem by applying the Schur complement to Lemma 1.

Theorem 1 *Suppose (A_e, B_e, C_e, D_e) is arbitrary but fixed and let $\gamma > 0$ be given. Then the filtering error system in (2.4) is stable and the $l_2 - l_\infty$ gain of the filtering error system is less than γ (4.7) if and only if there exists a matrix $0 < P \in \mathbb{R}^{2n \times 2n}$ such that*

$$\begin{bmatrix} \gamma^2 I & C_e P & D_e \\ P C_e^{\mathrm{T}} & P & 0 \\ D_e^{\mathrm{T}} & 0 & I \end{bmatrix} > 0, \tag{2.8}$$

$$\begin{bmatrix} P & A_e P & B_e \\ P A_e^{\mathrm{T}} & P & 0 \\ B_e^{\mathrm{T}} & 0 & I \end{bmatrix} > 0. \tag{2.9}$$

Proof: Equation (2.6) can be written as

$$-\gamma^2 I + D_e D_e^{\mathrm{T}} - (-C_e P)(-P^{-1})(-P C_e^{\mathrm{T}}) < 0. \tag{2.10}$$

Using the Schur complement, we obtain

$$\begin{bmatrix} -\gamma^2 I + D_e D_e^{\mathrm{T}} & (-C_e P) \\ (-P C_e^{\mathrm{T}}) & -P \end{bmatrix} < 0, \tag{2.11}$$

which can be further rewritten as

$$\begin{bmatrix} -\gamma^2 I & (-C_e P) \\ (-P C_e^{\mathrm{T}}) & -P \end{bmatrix} - \begin{bmatrix} -D_e \\ 0 \end{bmatrix} \begin{bmatrix} -I \end{bmatrix} \begin{bmatrix} -D_e^{\mathrm{T}} & 0 \end{bmatrix} < 0. \tag{2.12}$$

Applying the Schur complement to the above inequality, we obtain

$$\begin{bmatrix} -\gamma^2 I & -C_e P & -D_e \\ -P C_e^{\mathrm{T}} & -P & 0 \\ -D_e^{\mathrm{T}} & 0 & -I \end{bmatrix} < 0, \tag{2.13}$$

which proves (2.8).

By following the similar line and applying Schur complement, (2.9) can be proved. $\square$

16

Inequality (2.8) is nonlinear due to the product of variables. Hence, it cannot be directly solved using the LMI toolbox. In the following theorem, we transform the condition to LMIs with nonconvex constraints, which can be efficiently solved by using the product reduction algorithm (PRA) [63].

Theorem 2 *Let $\gamma > 0$ be given. Then there exists an admissible $l_2 - l_\infty$ deconvolution filter if and only if there exist matrices $P > 0$ and $W > 0$ such that*

$$\begin{bmatrix} \gamma^2 I & C_e & D_e \\ C_e^T & W & 0 \\ D_e^T & 0 & I \end{bmatrix} > 0, \tag{2.14}$$

$$\begin{bmatrix} P & A_e & B_e \\ A_e^T & W & 0 \\ B_e^T & 0 & I \end{bmatrix} > 0, \tag{2.15}$$

with nonconvex constraint

$$PW = I. \tag{2.16}$$

Proof: Multiplying (2.8) and (2.9) by $\mathrm{diag}\{I, P^{-1}, I\}$ to the left, and by $\mathrm{diag}\{I, P^{-1}, I\}^T$ to the right, respectively, we get (2.14) and (2.15). □

Remark 1: Inequality (2.9) does not have the product of variables and it is an LMI. Hence, the transformation from inequality (2.9) to (2.15) is actually not necessary.

Here, to facilitate the use of LMI toolbox to solve the problem, C_e and D_e can be written as

$$\begin{aligned} C_e &= \begin{bmatrix} C_s - D_f D_c C_s & -D_f C_c & -C_f \end{bmatrix} \\ &= \begin{bmatrix} C_s & 0 & 0 \end{bmatrix} + D_f \begin{bmatrix} -D_c C_s & -C_c & 0 \end{bmatrix} + C_f \begin{bmatrix} 0 & 0 & -I \end{bmatrix}, \\ D_e &= \begin{bmatrix} D_s - D_f D_c D_s & -D_f \end{bmatrix}, \\ &= \begin{bmatrix} D_s & 0 \end{bmatrix} + D_f \begin{bmatrix} -D_c C_s & -I \end{bmatrix}. \end{aligned} \tag{2.17}$$

respectively.

Corollary 1 *The FIR $l_2 - l_\infty$ deconvolution filter for system (2.4) can be designed by solving the following optimization problem:*

$$\min \gamma \quad subject \ to \ (2.14), \ (2.15), \ and \ (2.16).$$

2.4 Design Examples

In this section, design examples are given to illustrate the proposed algorithm. Suppose that the system shown in Figure 1 has the signal model $\sum_s$ with the following system matrices:

$$A_s^{\mathrm{T}} = \begin{bmatrix} 3.6015 & 1 & 0 & 0 & 0 & 0 \\ -5.6805 & 0 & 1 & 0 & 0 & 0 \\ 5.0232 & 0 & 0 & 1 & 0 & 0 \\ -2.6253 & 0 & 0 & 0 & 1 & 0 \\ 0.7707 & 0 & 0 & 0 & 0 & 1 \\ 0.0997 & 0 & 0 & 0 & 0 & 0 \end{bmatrix},$$

$$B_s = \begin{bmatrix} 1 \\ 0 \\ 0 \\ 0 \\ 0 \\ 0 \end{bmatrix},$$

$$C_s = \begin{bmatrix} 0.0002 & 0.0091 & 0.0323 & 0.0222 & 0.0029 & 0 \end{bmatrix},$$

$$D_s = 0,$$

and the channel model $\sum_c$ with the following system matrices

$$A_c = \begin{bmatrix} 1.6047 & 0.8520 & 0.1496 \\ 1 & 0 & 0 \\ 0 & 0 & 1 \end{bmatrix},$$

$$B_c = \begin{bmatrix} 1 \\ 0 \\ 0 \end{bmatrix},$$

$$C_c = \begin{bmatrix} -0.1747 & 0.2772 & 0.1135 \end{bmatrix},$$

$$D_c = 0.45.$$

In addition, assume, to start, that there is no channel noise (i.e., $v = 0$).

18

Example 1: $n_f = 6$. n_f is chosen to be 6. By using Corollary 1, $\gamma = 0.076$ is finally achieved, and the designed filter has the following system matrices:

$$C_f = \begin{bmatrix} -0.0122 & -0.1631 & -0.3451 & -0.2215 & 0.4250 & 1.2304 \end{bmatrix},$$

$$D_f = 1.9792.$$

The simulation results are shown in Figure 2.2, and the signal reconstruction error is illustrated in Figure 2.3. Further, a white noise with power of 1×10^{-4} is added and the results are shown in Figure 2.4, and accordingly the signal reconstruction error is shown in 2.5.
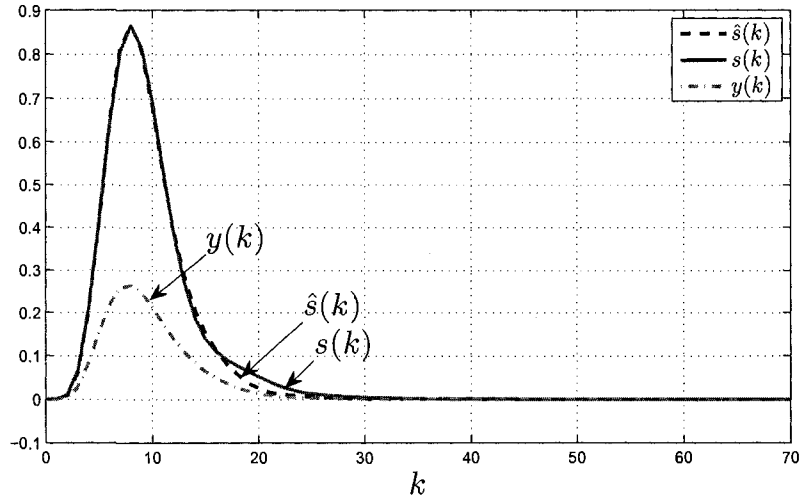
Figure 2.2: Example 1: Simulation results without channel noise ($n_f = 6$).

Example 2: $n_f = 15$. In the second example, the filter length is chosen larger. The suboptimal $\gamma = 0.07$ can be obtained by using Theorem 1 and the system matrices of the FIR filter are

$$C_f = \begin{bmatrix} -0.0039 & 0.0046 & 0.0192 & 0.0350 & 0.0442 & 0.0376 & 0.0084 & -0.0418 & -0.0989 \\ & & -0.1382 & -0.1329 & -0.0658 & 0.0623 & 0.2352 & 0.4391 \end{bmatrix},$$

19
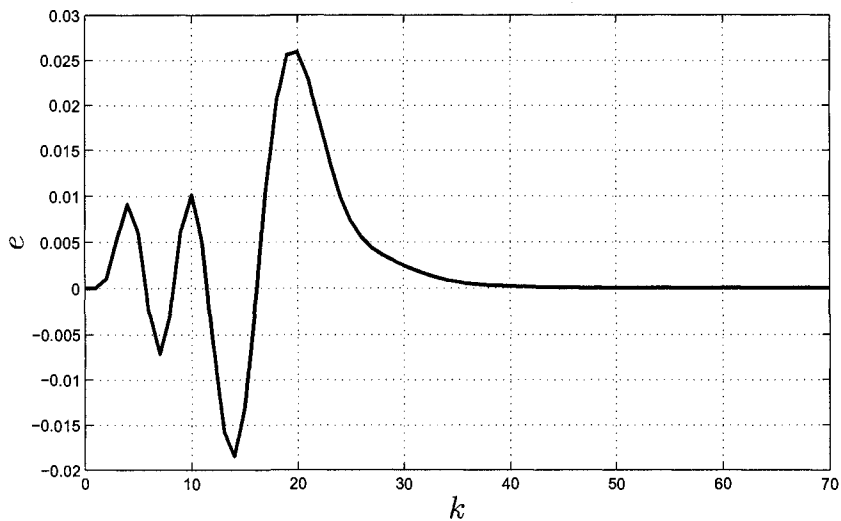
Figure 2.3: Example 1: Reconstruction error signal without channel noise ($n_f = 6$).
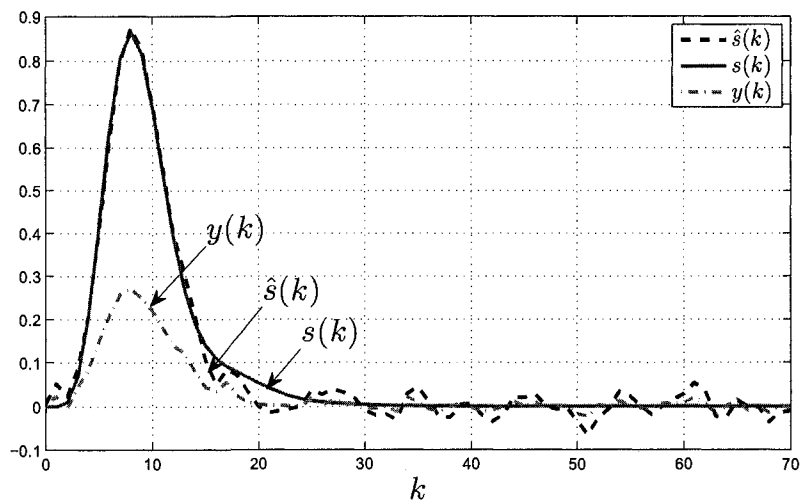
Figure 2.4: Example 1: Simulation results with channel noise ($n_f = 6$).

$$D_f = 2.5748.$$

The simulation results are shown in Figures 2.6 and 2.7. Then, a white noise with power of 1×10^{-4} is added and the results are shown in Figures 2.8 and 2.9.

20
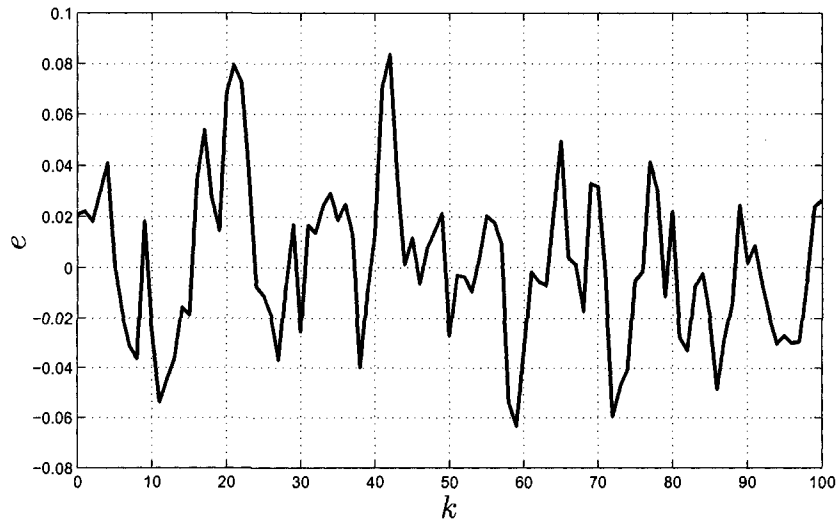
Figure 2.5: Example 1: Reconstruction error signal with channel noise ($n_f = 6$).
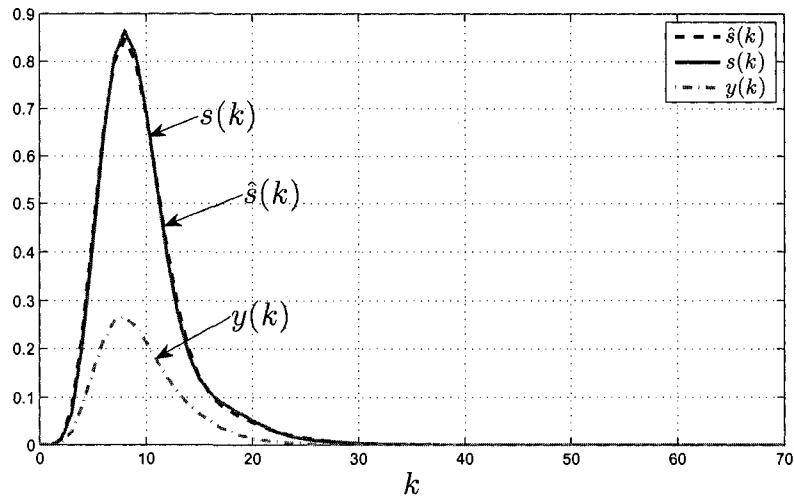
Figure 2.6: Example 2: Simulation results without channel noise ($n_f = 15$).

To take a closer look and make comparisons, we show the signal reconstruction errors of Example 1 and Example 2 in Figures 2.10 and 2.11, respectively. It is observed that for longer n_f the deconvolution filter provides better reconstruction

21
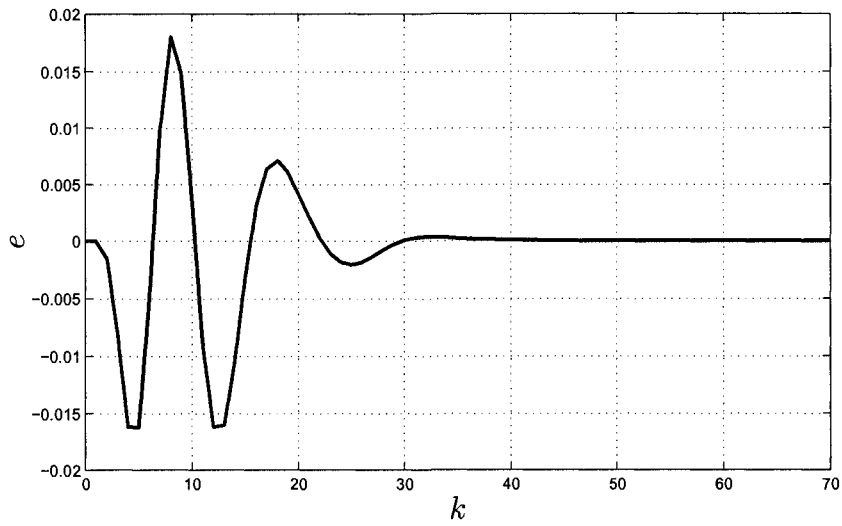
Figure 2.7: Example 2: Reconstruction error signal without channel noise ($n_f = 15$).
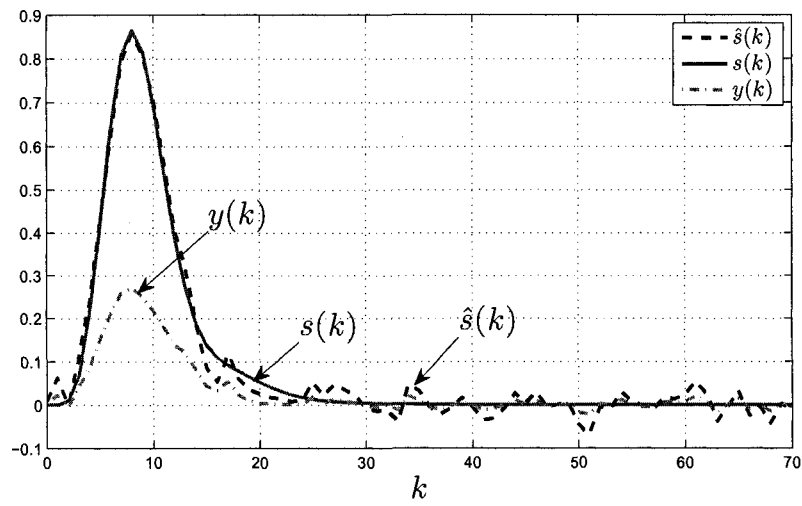
Figure 2.8: Example 2: Simulation results with channel noise ($n_f = 15$).

performance.
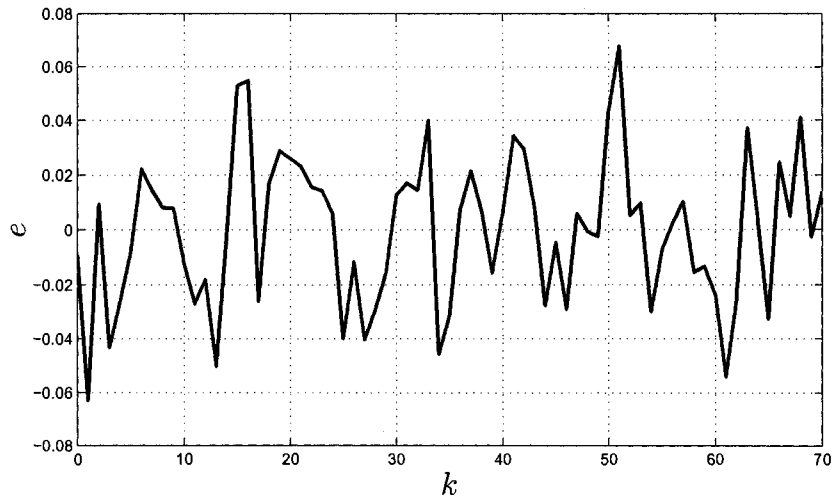
Figure 2.9: Example 2: Reconstruction error signal with channel noise ($n_f = 15$).
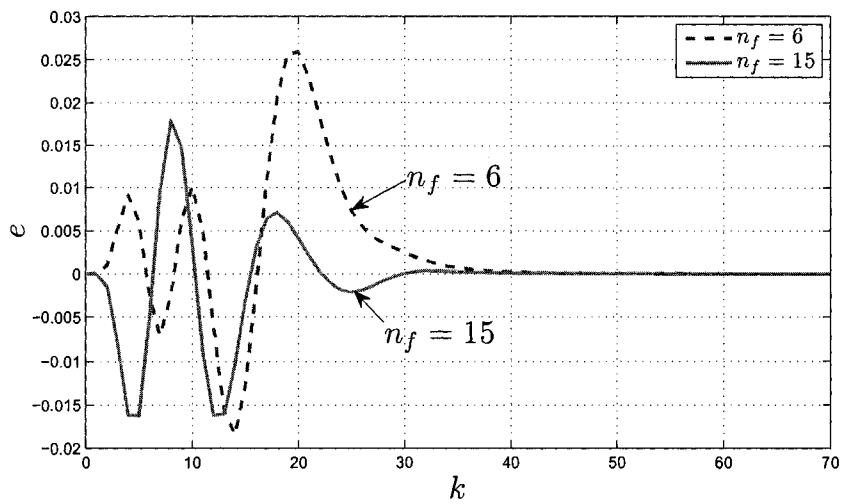
Figure 2.10: Comparison of reconstruction error signal without channel noise.

2.5 Conclusion

In this chapter, an LMI-based optimization approach and the PRA method are applied to design FIR deconvolution filters that guarantee the energy-to-peak per-
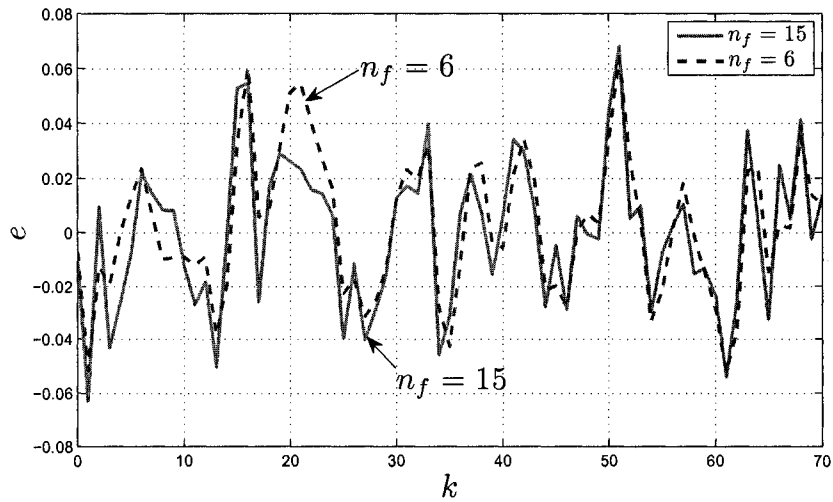
Figure 2.11: Comparison of reconstruction error signal with channel noise.

formance. Simulation examples illustrate the effectiveness of the proposed method; comparison studies show that for FIR filters, the longer the filter length, the better the performance.

On the other hand, however, the longer the filter length, more implementation cost will arise for the application. This posts a question worth to further research: Can an algorithm simultaneously design both the filter parameters and the filter length? To our best knowledge, such work is still an open topic and could be considered a future research problem.

Chapter 3

IIR Deconvolution Filter Design with Guaranteed Energy-to-Peak Performance

3.1 Introduction

In signal processing, many filter design problems often can be cast as a constrained optimization problem. This methodology has been applied to IIR filter design, e.g. [61, 49]. Particularly, the $\mathcal{H}_\infty$ optimization technique was used for the design of IIR filters considering the time-domain envelop constraints in [61]. Further, it was extended to deconvolution filter design in [49] by following a similar line. To the best of our knowledge, the $l_2 - l_\infty$ IIR deconvolution filter design has received less attention, which is the focus of this chapter.

The rest of the chapter is organized in the following way. We first formulate the IIR deconvolution filtering problem and state the objective of $l_2 - l_\infty$ filtering design in Section 3.2. In Section 3.3, the sufficient and necessary condition is derived to guarantee the $l_2 - l_\infty$ filtering performance. Further, the condition is transformed to LMIs. To illustrate the effectiveness of the proposed method, design examples are given in Section 3.4. Finally, the conclusion remarks are addressed in Section 3.5.

3.2 Problem Formulation

Consider the deconvolution filtering system shown in Figure 3.1. In the system, the source signal $s(k) \in \mathcal{R}$ is assumed to be generated by the signal model
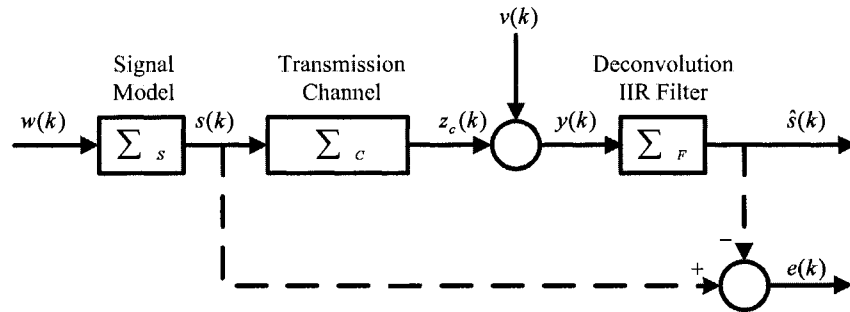
Figure 3.1: An IIR deconvolution filtering system model.

$$\sum S : \begin{cases} x_s(k+1) &=& A_s x_s(k) + B_s w(k) \\ s(k) &=& C_s x_s(k) + D_s w(k) \end{cases}, \tag{3.1}$$

where $x_s(k) \in \mathbb{R}^{n_s}$ is the model state vector, $w(k) \in l_2[0, \infty)$ is the driving signal of the model, and A_s, B_s, C_s, and D_s are known constant matrices of appropriate dimensions. The source signal is transmitted through a channel modeled by

$$\sum C : \begin{cases} x_c(k+1) &=& A_c x_c(k) + B_c s(k) \\ z_c(k) &=& C_c x_c(k) + D_c s(k), \end{cases}, \tag{3.2}$$

where $x_c(k) \in \mathbb{R}^{n_c}$ is the channel state vector.

At the receiving end, the measured signal $y(k)$ is equal to $z_c(k) + v(k)$, where $v(k)$ is the energy-bounded channel noise. To optimally recover the source signal $s(k)$, the signal $y(k)$ is deconvoluted by an IIR filter with the following state-space model

$$\sum F : \begin{cases} x_f(k+1) &=& A_f x_f(k) + B_f y(k) \\ \hat{s}(k) &=& C_f x_f(k) + D_f y(k) \end{cases}, \tag{3.3}$$

where $x_f(k) \in \mathbb{R}^{n_f}$ is the filter state vector, and A_f, B_f, C_f, and D_f are constant matrices to be designed.

Combining (3.1), (3.2), and augmenting the state vector give rise to the following state-space model:

$$\begin{cases} x(k+1) &=& Ax(k) + Bw_e(k) \\ y(k) &=& Cx(k) + Dw_e(k) \end{cases}, \tag{3.4}$$

where $x^{\mathrm{T}}(k) = \begin{bmatrix} x_s^{\mathrm{T}}(k), & x_c^{\mathrm{T}}(k) \end{bmatrix}$, $w_e^{\mathrm{T}}(k) = \begin{bmatrix} w^{\mathrm{T}}(k), & v^{\mathrm{T}}(k) \end{bmatrix}$ and the new system matrices are

$$A = \begin{bmatrix} A_s & 0 \\ B_c C_s & A_c \end{bmatrix},$$

$$B = \begin{bmatrix} B_s & 0 \\ B_c D_s & 0 \end{bmatrix},$$

$$C = \begin{bmatrix} D_c C_s & C_c \end{bmatrix},$$

$$D = \begin{bmatrix} D_c D_s & 1 \end{bmatrix}.$$

Define the filtering error as

$$e(k) = s(k) - \hat{s}(k).$$

Then the filtering error system can be represented by

$$\sum e : \begin{cases} x_e(k+1) &= A_e x_e(k) + B_e w_e(k) \\ e(k) &= C_e x_e(k) + D_e w_e(k) \end{cases},$$ (3.5)

where $x_e^{\mathrm{T}}(k) = \begin{bmatrix} x^{\mathrm{T}}(k), & x_f^{\mathrm{T}}(k) \end{bmatrix}$.

Considering that

$$\begin{aligned} s(k) &= C_s x_s(k) + D_s \omega(k) \\ &= \overbrace{\begin{bmatrix} C_s & 0 \end{bmatrix}}^{\Phi} \begin{bmatrix} x_s(k) \\ x_c(k) \end{bmatrix} + \overbrace{\begin{bmatrix} D_s & 0 \end{bmatrix}}^{\Gamma} \begin{bmatrix} \omega(k) \\ v(k) \end{bmatrix}, \end{aligned}$$

then we have

$$\begin{aligned} A_e &= \begin{bmatrix} A & 0 \\ B_f C & A_f \end{bmatrix}, \\ B_e &= \begin{bmatrix} B \\ B_f D \end{bmatrix}, \\ C_e &= \begin{bmatrix} \Phi - D_f C & -C_f \end{bmatrix}, \\ D_e &= \Gamma - D_f D. \end{aligned}$$

The main objective of this work is to develop the $l_2 - l_\infty$ IIR filter of the form in (3.3) such that:

1. The filtering error system is stable.

2. The filtering error system guarantees

$$\|e\|_\infty \leqslant \gamma \|w_e\|_2$$

for all nonzero $w_e \in l_2[0, \infty)$, where $\|w_e\|_2^2 := \sum_{k=0}^{\infty} w_e^{\mathrm{T}}(k) w_e(k)$ and $\|e\|_\infty^2 = \sup_k e^{\mathrm{T}}(k) e(k)$.

28

3.3 IIR $l_2 - l_\infty$ Filter Design

In this section, we will formulate and solve the $l_2 - l_\infty$ IIR filter design problem under the framework of LMI. Lemma 1 and Theorem 1 stated in Chapter 2 also hold for the case of IIR deconvolution filter design, except the different definitions for the involved matrices A_e, B_e, C_e, and D_e. To make the presentation concise, we choose not to reiterate the results here, but just to cite Lemma 1 and Theorem 1 for the following derivation.

Theorem 3 *Suppose (A_e, B_e, C_e, D_e) is arbitrary but fixed and let $\gamma > 0$ be given. Then the filtering error system in (3.5) is stable and the $l_2 - l_\infty$ gain of the filtering error system is less than γ if and only if there exist $Z > 0$, $Y > 0$, Q, F, G, D_f (with appropriate dimensions) such that*

$$
\begin{bmatrix}
\gamma^2 I & \Phi - D_f C - G & \Phi - D_f C & \Gamma - D_f D \\
* & Z & Z & 0 \\
* & * & Y & 0 \\
* & * & * & I
\end{bmatrix} > 0, \qquad (3.6)
$$

$$
\begin{bmatrix}
Z & Z & ZA & ZA & ZB \\
* & Y & YA + FC + Q & YA + FC & YB + FD \\
* & * & Z & Z & 0 \\
* & * & * & Y & 0 \\
* & * & * & * & I
\end{bmatrix} > 0. \qquad (3.7)
$$

Here, $*$ represents an ellipsis for the terms that are introduced by symmetry. Further, the system matrices of the deconvolution IIR filter are given by

$$
\begin{aligned}
A_f &= (Z - Y)^{-1} Q, \\
B_f &= (Z - Y)^{-1} F, \qquad (3.8) \\
C_f &= G.
\end{aligned}
$$

Proof: Let us partition P in (2.8) and (2.9) and its inverse as

$$
P = \begin{bmatrix} X & U \\ * & \hat{X} \end{bmatrix}, \quad P^{-1} = \begin{bmatrix} Y & V \\ * & \hat{Y} \end{bmatrix}, \qquad (3.9)
$$

where X, Y and $\hat{X}, \hat{Y}$ are all symmetric and positive definite matrices. Then we have

$$PP^{-1} = \begin{bmatrix} XY + UV^{\mathrm{T}} & XV + U\hat{Y} \\ U^{\mathrm{T}}Y + \hat{X}V^{\mathrm{T}} & U^{\mathrm{T}}V + \hat{X}\hat{Y} \end{bmatrix} = \begin{bmatrix} I & 0 \\ 0 & I \end{bmatrix}. \tag{3.10}$$

From this partition of matrix P, we can obtain the following one-to-one change of variable:

$$\begin{aligned}
\begin{bmatrix} A_f & B_f \\ C_f & 0 \end{bmatrix} &= \begin{bmatrix} V & 0 \\ 0 & I \end{bmatrix}^{-1} \begin{bmatrix} Q & F \\ G & 0 \end{bmatrix} \begin{bmatrix} U^{\mathrm{T}}X^{-1} & 0 \\ 0 & I \end{bmatrix}^{-1} \\
&= \begin{bmatrix} V^{-1} & 0 \\ 0 & I \end{bmatrix}^{-1} \begin{bmatrix} Q & F \\ G & 0 \end{bmatrix} \begin{bmatrix} XU^{-\mathrm{T}} & 0 \\ 0 & I \end{bmatrix}^{-1} \\
&= \begin{bmatrix} V^{-1}QXU^{-\mathrm{T}} & V^{-1}F \\ GXU^{-\mathrm{T}} & 0 \end{bmatrix}.
\end{aligned} \tag{3.11}$$

where the indicated inverses exist due to the fact that X is symmetric and positive definite and matrices V and U are both nonsingular.

Using the partition P in (3.9),

$$\tilde{C}P = \begin{bmatrix} \Phi - D_f C & -C_f \end{bmatrix} \begin{bmatrix} X & U \\ U^{\mathrm{T}} & \hat{X} \end{bmatrix} = \begin{bmatrix} (\Phi - D_f C)X - C_f U^{\mathrm{T}} & (\Phi - D_f C)U - C_f \hat{X} \end{bmatrix}.$$

Inequality (2.8) becomes

$$\begin{bmatrix} \gamma^2 I & \tilde{C} & \tilde{D} \\ \tilde{C}^{\mathrm{T}} & W & 0 \\ \tilde{D}^{\mathrm{T}} & 0 & I \end{bmatrix} = \begin{bmatrix} \gamma^2 I & (\Phi - D_f C)X - C_f U^{\mathrm{T}} & (\Phi - D_f C)U - C_f \hat{X} & \Gamma - D_f D \\ * & X & U & 0 \\ * & * & \hat{X} & 0 \\ * & * & * & I \end{bmatrix}. \tag{3.12}$$

Defining the square and full rank matrix

$$\tilde{J} = \begin{bmatrix} X^{-1} & Y \\ 0 & V^{\mathrm{T}} \end{bmatrix} \quad and \quad \tilde{J}^{\mathrm{T}} = \begin{bmatrix} X^{-1} & 0 \\ Y & V \end{bmatrix} \tag{3.13}$$

and multiplying inequality (2.8) to the left by the full rank matrix $J^{\mathrm{T}} = \mathrm{diag}[I, \tilde{J}^{\mathrm{T}}, I]$ and to the right by J and considering the equalities in (3.10) and (3.11) provide the following inequality

$$\begin{bmatrix} \gamma^2 I & \Phi - D_f C - G & \Phi - D_f C & \Gamma - D_f D \\ * & X^{-1} & X^{-1} & 0 \\ * & * & Y & 0 \\ * & * & * & I \end{bmatrix} > 0. \tag{3.14}$$

30

Using a similar procedure and multiplying inequality (2.9) to the left by the full rank matrix $J^{\mathrm{T}} = \mathrm{diag}[\tilde{J}^{\mathrm{T}}, \tilde{J}^{\mathrm{T}}, I]$ and to the right by J provide the following inequality

$$\begin{bmatrix} X^{-1} & X^{-1} & X^{-1}A & X^{-1}A & X^{-1}B \\ * & Y & YA+FC+Q & YA+FC & YB+FD \\ * & * & X^{-1} & X^{-1} & 0 \\ * & * & * & Y & 0 \\ * & * & * & * & I \end{bmatrix} > 0. \qquad (3.15)$$

Let $X^{-1} = Z$, we can obtain the theorem. Let $U = X = Z^{-1}$, so U is nonsingular. Then, from $XY + UV^{\mathrm{T}} = I$, we can get

$$V^{\mathrm{T}} = Z(I - XY) \Rightarrow V = (I - YX)Z = Z - YXZ = Z - Y.$$

Hence,

$$\begin{aligned} A_f &= V^{-1}QZ^{-1}Z = V^{-1}Q = (Z-Y)^{-1}Q, \\ B_f &= V^{-1}F = (Z-Y)^{-1}F, \\ C_f &= GXX^{-1} = G. \end{aligned}$$

This completes the proof. $\qquad\qquad\qquad\qquad\qquad\qquad\qquad\qquad \square$

Corollary 2 *The IIR $l_2 - l_\infty$ deconvolution filter can be found by solving the following optimization problem:*

$$\min \quad \gamma \quad subject\ to\ (3.6)\ and\ (3.7). \qquad (3.16)$$

3.4   Design Examples

In this section, a design example is given to illustrate the proposed algorithm. Also its performance will be compared to that of the FIR deconvolution filter designed in Chapter 2.

Example 1: Suppose that the system shown in Figure 3.1 has the signal model $\sum_s$

with the following system matrices

$$
A_s^{\mathrm{T}} = \begin{bmatrix}
3.6015 & 1 & 0 & 0 & 0 & 0 \\
-5.6805 & 0 & 1 & 0 & 0 & 0 \\
5.0232 & 0 & 0 & 1 & 0 & 0 \\
-2.6253 & 0 & 0 & 0 & 1 & 0 \\
0.7707 & 0 & 0 & 0 & 0 & 1 \\
0.0997 & 0 & 0 & 0 & 0 & 0
\end{bmatrix},
$$

$$
B_s = \begin{bmatrix} 1 \\ 0 \\ 0 \\ 0 \\ 0 \\ 0 \end{bmatrix},
$$

$$
C_s = \begin{bmatrix} 0.0002 & 0.0091 & 0.0323 & 0.0222 & 0.0029 & 0 \end{bmatrix},
$$

$$
D_s = 0,
$$

and the channel model $\sum_c$ with the following system matrices

$$
A_c = \begin{bmatrix}
1.6047 & 0.8520 & 0.1496 \\
1 & 0 & 0 \\
0 & 0 & 1
\end{bmatrix},
$$

$$
B_c = \begin{bmatrix} 1 \\ 0 \\ 0 \end{bmatrix},
$$

$$
C_c = \begin{bmatrix} -0.1747 & 0.2772 & 0.1135 \end{bmatrix},
$$

$$
D_c = 0.45.
$$

Then, applying Corollary 2, $\gamma = 2.4702 \times 10^{-5}$ is obtained, and the system

matrices of the designed IIR deconvolution filter are:

$$
A_f = \begin{bmatrix}
2.8726 & -8.9068 & -16.04 & -33.634 & -5.3168 \\
0.7098 & -1.9377 & -9.7485 & -14.016 & -2.1392 \\
-0.0023335 & 0.093794 & -2.5909 & -3.3499 & -0.25561 \\
-0.0049231 & -0.02528 & 0.70658 & 0.42721 & -0.0077303 \\
0.001806 & 0.016532 & 0.12752 & 0.87206 & 0.0048452 \\
-0.0006155 & -0.0057867 & -0.043863 & 0.043022 & 0.99833 \\
-2.7865 \times 10^{-7} & 2.3522 \times 10^{-6} & 7.0543 \times 10^{-7} & 4.7742 \times 10^{-5} & 1.0646 \times 10^{-5} \\
-8.2242 \times 10^{-8} & 6.0906 \times 10^{-7} & -1.0144 \times 10^{-7} & 1.3258 \times 10^{-5} & 2.8579 \times 10^{-6} \\
-1.6269 \times 10^{-7} & 1.6791 \times 10^{-6} & 1.7527 \times 10^{-6} & 2.7742 \times 10^{-5} & 6.346 \times 10^{-6}
\end{bmatrix}
$$

$$\begin{bmatrix}
-12.648 & 602.51 & -824.15 & 291.99 \\
-5.0263 & 258.4 & -358.52 & 129.05 \\
-0.73913 & 54.618 & -79.568 & 30.135 \\
0.30907 & -6.1404 & 6.75 & -1.7328 \\
-0.10622 & 1.787 & -1.8061 & 0.38496 \\
0.036067 & -0.60002 & 0.60247 & -0.12626 \\
2.6653 \times 10^{-5} & 1.992 & -1.4669 & 0.40146 \\
7.4824 \times 10^{-6} & 0.99975 & 0.00030928 & -9.8384 \times 10^{-5} \\
1.5063 \times 10^{-5} & -0.00052254 & 1.0007 & -0.00021386
\end{bmatrix}$$

$$B_f = \begin{bmatrix}
1183.8 \\
595.79 \\
191.29 \\
16.065 \\
-7.384 \\
2.5475 \\
2.2222 \\
1.3048 \times 10^{-5} \\
-9.194 \times 10^{-5}
\end{bmatrix},$$

$$C_f = \begin{bmatrix} 1.0694 \times 10^{-9} & -8.354 \times 10^{-8} & -2.5119 \times 10^{-7} & 8.504 \times 10^{-7} & 3.6416 \times 10^{-7} \end{bmatrix}$$
$$6.2363 \times 10^{-7} \quad 0.3882 \quad -0.61598 \quad 0.25222 \,],$$

$$D_f = 2.2222.$$

Figure 3.2 shows the filter output $\hat{s}(k)$, signals $s(k)$ and $y(k)$, when no channel noise $v(k)$ is added. In this case, the reconstruction error signal is illustrated in Figure 3.3.

Then, a white noise with power of 1×10^{-4} is added and the results are shown in Figures 3.4 and 3.5.

Example 2: Comparison between IIR and FIR deconvolution filter design. To compare the performance of the IIR deconvolution filter and the FIR one ($n_f = 15$), we illustrate their signal reconstruction errors, for the case of adding noise (Figure 3.6) and without adding noise (Figure 3.7), respectively. From Figure 3.6, it is observed that the IIR deconvolution filter obviously outperforms the FIR one.
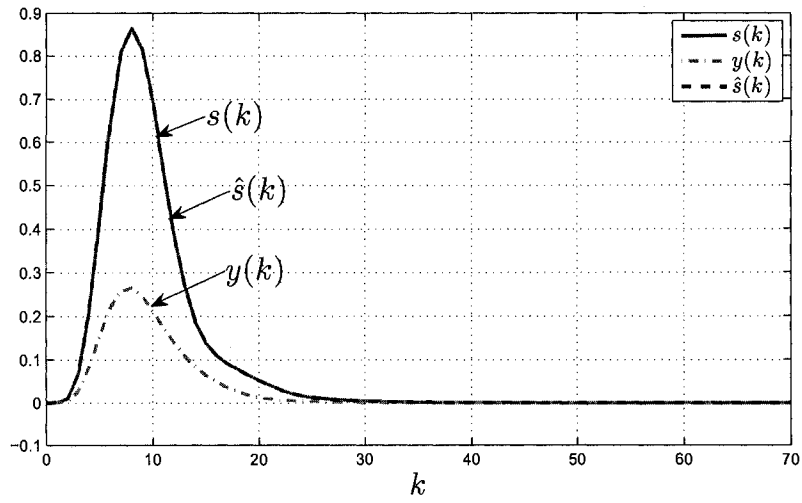
Figure 3.2: Simulation results without channel noise.
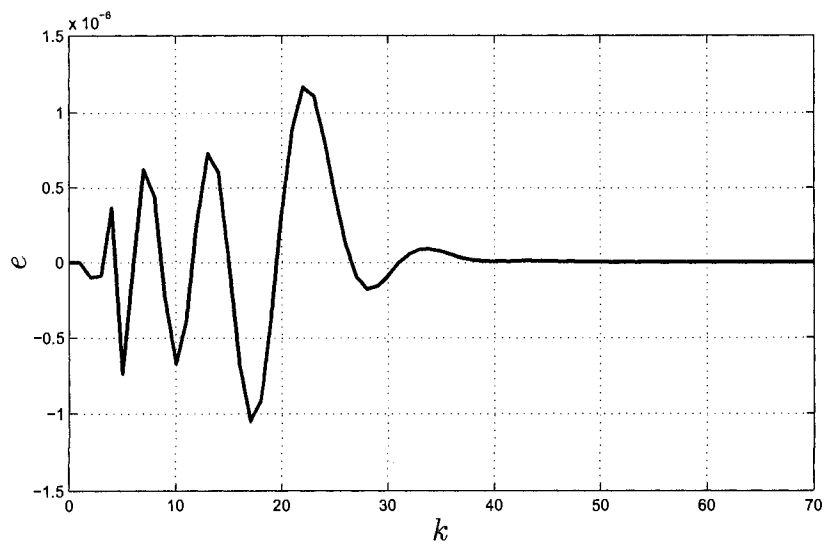
Figure 3.3: Reconstruction error signal without channel noise.

3.5 Conclusion

In this chapter, we developed the $l_2 - l_\infty$ IIR deconvolution filters by using the LMI technique. Design examples verify that the proposed method has good performance

34
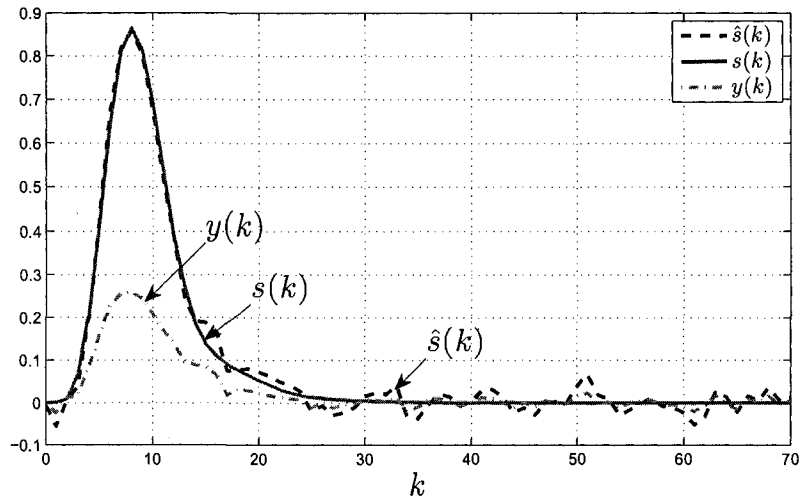
Figure 3.4: Simulation results with channel noise.
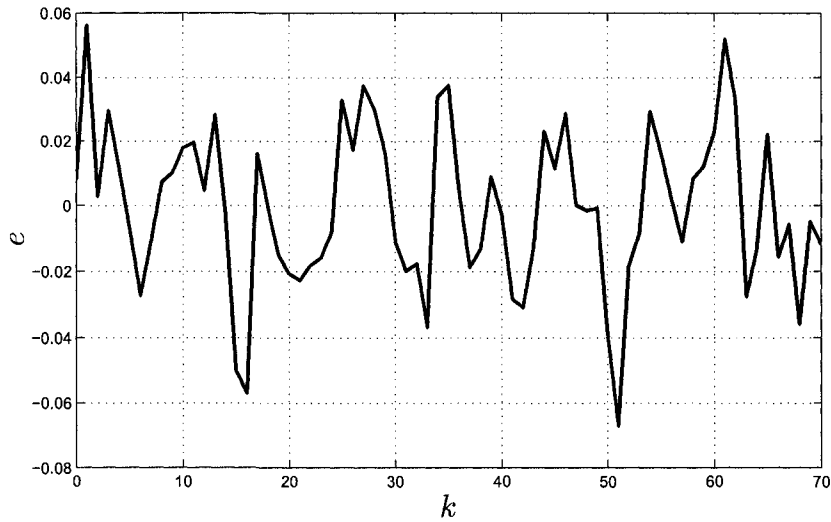
Figure 3.5: Reconstruction error signal with channel noise.

in terms of the observed small signal reconstruction errors. The developed IIR filter is also compared to the FIR one proposed in Chapter 2, and it is observed that the IIR filter outperforms the FIR one under the situation of no noise. One way to
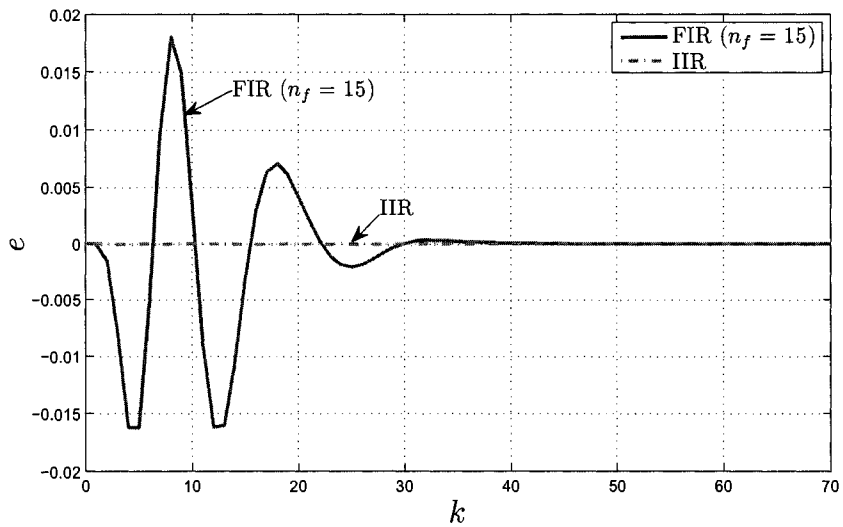
Figure 3.6: Comparison of signal reconstruction errors without channel noise.
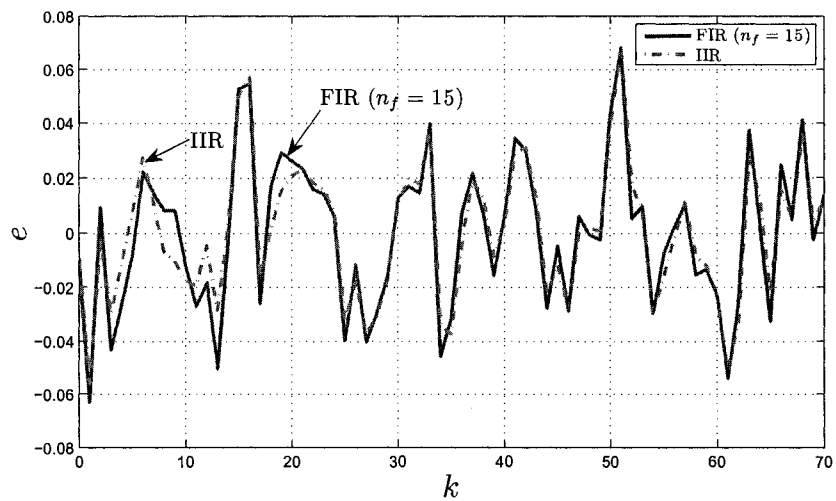
Figure 3.7: Comparison of signal reconstruction errors with channel noise.

improve the performance of FIR deconvolution filters is to increase the filter length.

Chapter 4

Robust IIR Deconvolution Filter Design with Guaranteed Energy-to-Peak Performance

4.1 Introduction

In practice, there is still another important factor to take care of for the deconvo-
lution filter design – channel uncertainties. In literature, the channel uncertainties
have received relatively less attention. In [49, 48, 50, 61], channel uncertainties were
not considered. In [25], the uncertainties in the channel were formulated as satis-
fying the integral quadratic constraints (IQCs), and further developed the robust
FIR deconvolution filters. Another effective way to characterize the channel uncer-
tainties is the polytopic uncertainty description that has been widely used in the
area of control and estimation. In this chapter, we focus on the robust design of IIR
deconvolution filters considering the polytopic uncertainties in the channel.

The rest of the chapter is organized in the following way. We first formulate
the robust IIR filtering problem and state the objective of robust $l_2 - l_\infty$ filtering
design in Section 4.2. In Section 4.3, the sufficient condition is derived to guarantee
the robust $l_2 - l_\infty$ filtering performance. Further, to decrease the conservativeness
of the design, the parameter-dependent design method is introduced. The derived
conditions are further transformed to LMIs. To illustrate the effectiveness of the
proposed methods, design examples are given in Section 4.4. Finally, the concluding
remarks are given in Section 4.5.

4.2 Problem Formulation

To characterize the uncertainties on the channel model, we introduce the polytopic
uncertainties description: Assume that the system matrices of the channel model
belong to a convex polytopic set defined as

$$(A_c, B_c, C_c, D_c) := \left\{ \begin{bmatrix} A_c(\alpha) & B_c(\alpha) \\ C_c(\alpha) & D_c(\alpha) \end{bmatrix} = \sum_{i=1}^{s} \alpha_i \begin{bmatrix} A_{ci} & B_{ci} \\ C_{ci} & D_{ci} \end{bmatrix}, \alpha \in \Upsilon \right\}, \quad (4.1)$$

where Υ is the unit simplex

$$\Upsilon = \left\{ (\alpha_1, \cdots, \alpha_s) : \sum_{i=1}^{s} \alpha_i = 1, \alpha_i \geq 0 \right\}.$$

The state-space model of the IIR filter to be designed takes the same form as (3.3) in Chapter 3.

For the state-space model (3.4) by combining (3.1), (3.2), and augmenting the state vector, its system matrices (A, B, C, D) are with the following polytopic uncertainties accordingly:

$$(A, B, C, D) := \left\{ \begin{bmatrix} A(\alpha) & B(\alpha) \\ C(\alpha) & D(\alpha) \end{bmatrix} = \sum_{i=1}^{s} \alpha_i \begin{bmatrix} A_i & B_i \\ C_i & D_i \end{bmatrix}, \alpha \in \Upsilon \right\}. \qquad (4.2)$$

The objective is to develop the robust $l_2 - l_\infty$ IIR filter of the form in (3.3) such that for all admissible uncertainties:

1. The filtering error system is stable.

2. The filtering error system guarantees

$$\|e\|_\infty \leqslant \gamma \|w_e\|_2$$

for all nonzero $w_e \in l_2[0, \infty)$, where $\|w_e\|_2^2 := \sum_{k=0}^{\infty} w_e^{\mathrm{T}}(k) w_e(k)$ and $\|e\|_\infty^2 = \sup_k e^{\mathrm{T}}(k) e(k)$.

4.3 Robust IIR $l_2 - l_\infty$ Filter Design

We can easily extend Theorem 3 in Chapter 3 to obtain sufficient conditions for the robust $l_2 - l_\infty$ deconvolution IIR filters with polytopic uncertainties, thanks to the inherent properties of the convex combination – it suffices to verify the constraints only at the vertices of the polytopic uncertain parameters.

Theorem 4 *Suppose (A_e, B_e, C_e, D_e) are arbitrary but fixed and let $\gamma > 0$ be given. Then the filtering error system in (3.5) is stable and the $l_2 - l_\infty$ gain of the filtering*

error system is less than γ (4.7), if there exist $Z > 0$, $Y > 0$, Q, F, G, D_f satisfying

$$\begin{bmatrix} \gamma^2 I & \Phi - D_f C_i - G & \Phi - D_f C_i & \Gamma - D_f D_i \\ * & Z & Z & 0 \\ * & * & Y & 0 \\ * & * & * & I \end{bmatrix} > 0, \qquad (4.3)$$

$$\begin{bmatrix} Z & Z & ZA_i & ZA_i & ZB_i \\ * & Y & YA_i + FC_i + Q & YA_i + FC_i & YB_i + FD_i \\ * & * & Z & Z & 0 \\ * & * & * & Y & 0 \\ * & * & * & * & I \end{bmatrix} > 0, \qquad (4.4)$$

where $i = 1, 2, \cdots, s$, and the filter is given by

$$\begin{aligned} A_f &= (Z - Y)^{-1} Q, \\ B_f &= (Z - Y)^{-1} F, \qquad (4.5) \\ C_f &= G. \end{aligned}$$

Proof: It can be readily proved by following the similar line of Theorem 3. $\square$

Corollary 3 *The robust IIR $l_2 - l_\infty$ filter can be found by solving the following optimization problem:*

$$\min \quad \gamma \;\; subject\; to\; (4.3)\; and\; (4.4),\; \forall i = 1, \ldots, s. \qquad (4.6)$$

Even though it is straightforward to obtain above results to design a robust $l_2 - l_\infty$ deconvolution filter, the design would be conservative in that the resulting $l_2 - l_\infty$ gain may not be small enough. How to develop a less conservative design method will be the focus in the following. In the literature, it has been reported that the parameter-dependent Lyapunov function method can effectively reduce the conservativeness in robust control [32] and robust filtering design [16]. In this work, we apply this method to the robust $l_2 - l_\infty$ deconvolution filter design.

For a clearer presentation here, we reiterate Lemma 1 for the IIR case, that is adapted from Lemma 7 in [18].

Lemma 2 *Suppose system matrices of the deconvolution IIR filter, (A_e, B_e, C_e, D_e) are arbitrary but fixed and let $\gamma > 0$ be given. Then the filtering error system is stable and the $l_2 - l_\infty$ gain of the filtering error system is less than γ, that is*

$$\sup_{0 \neq w \in l_2} \frac{\|e\|_\infty}{\|w\|_2} < \gamma, \tag{4.7}$$

if and only if there exists a matrix $Y > 0$ such that

$$C_e Y C_e^{\mathrm{T}} + D_e D_e^{\mathrm{T}} \quad < \quad \gamma^2 I \tag{4.8}$$

$$A_e Y A_e^{\mathrm{T}} + B_e B_e^{\mathrm{T}} \quad < \quad Y. \tag{4.9}$$

Proof: It can be proved by following the results in [18, 16]. □

The next theorem presents a new version of the $l_2 - l_\infty$ performance condition which is equivalent to Lemma 2.

Theorem 5 *Suppose (A_e, B_e, C_e, D_e) is arbitrary but fixed and let $\gamma > 0$ be given. Then the filtering error system in (2.4) is stable and the $l_2 - l_\infty$ gain of the filtering error system is less than γ (4.7) if and only if there exist $0 < Y$ and G satisfying*

$$\begin{bmatrix} \gamma^2 I & C_e G & D_e \\ * & G^{\mathrm{T}} + G - Y & 0 \\ * & * & I \end{bmatrix} > 0, \tag{4.10}$$

$$\begin{bmatrix} Y & A_e G & B_e \\ * & G^{\mathrm{T}} + G - Y & 0 \\ * & * & I \end{bmatrix} > 0. \tag{4.11}$$

Proof: By applying the Schur complement to (4.8) and (4.9) and by choosing $G = G^{\mathrm{T}} = Y$ we can obtain (4.10) and (4.11). On the other hand, assuming (4.10) and (4.11) are feasible, we explore the fact that $G + G^{\mathrm{T}} - Y > 0$, so that G is nonsingular and $(G^{\mathrm{T}} - Y)Y^{-1}(G - Y) \geq 0$ always holds. Hence, the inequality $G + G^{\mathrm{T}} - Y \leq G^{\mathrm{T}} Y^{-1} G$ enable us to conclude that

$$\begin{bmatrix} \gamma^2 I & C_e G & D_e \\ * & G^{\mathrm{T}} Y^{-1} G & 0 \\ * & * & I \end{bmatrix} > 0, \tag{4.12}$$

41

$$\begin{bmatrix} Y & A_e G & B_e \\ * & G^T Y^{-1} G & 0 \\ * & * & I \end{bmatrix} > 0. \qquad (4.13)$$

Performing congruence transformations to (4.12) and (4.13) by $\mathrm{diag}\{I, G^{-1}, I\}$ together with Schur complement operations yield (4.10) and (4.11), which conclude the proof. $\qquad\square$

Now, we are in a good position to give the main results on the robust $l_2 - l_\infty$ deconvolution filter design.

Theorem 6 *Suppose (A_e, B_e, C_e, D_e) is arbitrary but fixed and let $\gamma > 0$ be given. Then the filtering error system in (3.5) is stable and the $l_2 - l_\infty$ gain of the filtering error system is less than γ (4.7), if and only if there exist $0 < X$, $0 < V$, Z, R, F, M, N, T, D_f satisfying*

$$\begin{bmatrix} \gamma^2 I & \Phi - D_f C - T & \Phi - D_f C & \Gamma - D_f D \\ * & R^T + R - X & R^T + F + U^T - Z & 0 \\ * & * & F^T + F - V & 0 \\ * & * & * & I \end{bmatrix} > 0, \qquad (4.14)$$

$$\begin{bmatrix} X & Z & R^T A & R^T A & R^T B \\ * & V & F^T A + NC + M & F^T A + NC & F^T B + ND \\ * & * & R^T + R - X & R^T + F + U^T - Z & 0 \\ * & * & * & F^T + F - V & 0 \\ * & * & * & * & I \end{bmatrix} > 0, \qquad (4.15)$$

and the IIR filter is given by

$$\begin{aligned} A_f &= U^{-1} M \\ B_f &= U^{-1} N \qquad\qquad (4.16) \\ C_f &= T. \end{aligned}$$

Proof: The proof is in the appendix. $\qquad\square$

For polytopic uncertainties, we have the following results on the robust IIR $l_2 - l_\infty$ deconvolution filter design.

Theorem 7 *Let $\gamma > 0$ be given. Then the filtering error system in (3.5) is stable and the $l_2 - l_\infty$ gain of the filtering error system is less than γ (4.7), if there exist $0 < X_i,\ 0 < V_i,\ Z_i,\ i = 1, \ldots, s,\ R,\ F,\ M,\ N,\ T,\ D_f$ satisfying*

$$\begin{bmatrix} \gamma^2 I & \Phi - D_f C_i - T & \Phi - D_f C_i & \Gamma - D_f D_i \\ * & R^{\mathrm{T}} + R - X_i & R^{\mathrm{T}} + F + U^{\mathrm{T}} - Z_i & 0 \\ * & * & F^{\mathrm{T}} + F - V_i & 0 \\ * & * & * & I \end{bmatrix} > 0, \qquad (4.17)$$

$$\begin{bmatrix} X_i & Z_i & R^{\mathrm{T}} A_i & R^{\mathrm{T}} A_i & R^{\mathrm{T}} B_i \\ * & V_i & F^{\mathrm{T}} A_i + N C_i + M & F^{\mathrm{T}} A_i + N C_i & F^{\mathrm{T}} B_i + N D_i \\ * & * & R^{\mathrm{T}} + R - X_i & R^{\mathrm{T}} + F + U^{\mathrm{T}} - Z_i & 0 \\ * & * & * & F^{\mathrm{T}} + F - V_i & 0 \\ * & * & * & * & I \end{bmatrix} > 0. \quad (4.18)$$

and the IIR filter is given by (4.16).

Proof: It can be proved by following the similar procedure in Theorem 6. $\square$

Corollary 4 *The robust IIR $l_2 - l_\infty$ deconvolution filter can be found by solving the following optimization problem:*

$$\min \quad \gamma \quad subject\ to\ (4.17)\ and\ (4.18),\ \forall i = 1, \ldots, s. \qquad (4.19)$$

4.4 Design Examples

Example 1: First of all, it is worth mentioning that Theorem 3 in Chapter 3 is equivalent to Theorem 6, for systems without uncertainties. To verify this, applying the method in Theorem 6 to design the IIR deconvolution filter for the same system used in Chapter 3, $\gamma = 1.3045$ is obtained, which is identical to that obtained in Section 3.4 of Chapter 3.

Example 2: Robust $l_2 - l_\infty$ IIR deconvolution filter design. Next, we turn our attention back to the design for a system with polytopic uncertainties. The comparison simulations will show and verify that the parameter-dependent Lyapunov method achieves better performance.

Assume that the channel model has the polytopic uncertainty with following system matrices:

$$A_c = \begin{bmatrix} \alpha & 0.8520 & 0.1496 \\ 1 & 0 & 0 \\ 0 & 0 & 1 \end{bmatrix},$$

$$B_c = \begin{bmatrix} 1 \\ 0 \\ 0 \end{bmatrix},$$

$$C_c = \begin{bmatrix} -0.1747 & \beta & 0.1135 \end{bmatrix},$$

$$D_c = 0.45,$$

where

$$1.59 \leq \alpha \leq 1.61,$$

$$0.2771 \leq \beta \leq 0.2773.$$

First, we apply Corollary 3 to design the filter, and the resulting $l_2 - l_\infty$ gain is shown in Table 4.1. The corresponding system matrices of the designed filter are:

$$A_f = \begin{bmatrix} 3.0430 & -5.2312 & 3.1693 & -5.3758 & 2.9407 & -1.5944 & 13.5410 & -19.3616 & 7.2081 \\ 0.7642 & -0.1881 & -0.9689 & -2.1347 & 1.5106 & -1.0516 & 10.2480 & -14.8256 & 5.5830 \\ 0.0062 & 0.5199 & -0.4547 & -1.2623 & 0.7939 & -0.5770 & 6.6597 & -9.9013 & 3.8249 \\ -0.0188 & -0.0570 & 0.3038 & -0.1434 & 0.0861 & -0.1387 & 3.4499 & -5.4978 & 2.2507 \\ -0.0166 & 0.0520 & -0.4081 & 1.2562 & -0.2963 & 0.1828 & 1.1685 & -2.3430 & 1.1079 \\ -0.0389 & 0.2584 & -0.7043 & 1.1917 & -0.0824 & 0.5377 & -0.0056 & -0.6519 & 0.4595 \\ -0.0610 & 0.3661 & -0.9920 & 1.4940 & -1.2053 & 0.5255 & 1.5319 & -1.3268 & 0.5055 \\ -0.0712 & 0.4249 & -1.1397 & 1.6668 & -1.3417 & 0.5732 & 0.8597 & -0.3854 & 0.3301 \\ -0.0645 & 0.3897 & -1.0375 & 1.5208 & -1.2495 & 0.5343 & 0.2396 & 0.1079 & 0.5103 \end{bmatrix},$$

$$B_f = \begin{bmatrix} 137.6904 \\ 105.6959 \\ 69.8332 \\ 36.6473 \\ 12.0215 \\ -1.4010 \\ 2.7624 \\ 0.7167 \\ 0.0094 \end{bmatrix},$$

$$C_f = \begin{bmatrix} -0.0011 & -0.0023 & 0.0195 & -0.0196 & 0.0396 & -0.0086 & 0.1196 & -0.2597 & 0.1304 \end{bmatrix},$$

$$D_f = 1.9161.$$

44

Table 4.1: Comparison of performance using two different methods

$l_2 - l_\infty$ gain	Direct method (Corollary 3)	Parameter-dependent Lyapunov function method (Corollary 4)
γ	0.28175	0.1751

Figure 4.1 shows the filter output $\hat{s}(k)$, signals $s(k)$, and $y(k)$ without channel noise $v(k)$. The reconstructed error signal is shown in Figure 4.2. Then, a white noise with power of 1×10^{-4} is added and the results are shown in Figures 4.3 and 4.4.
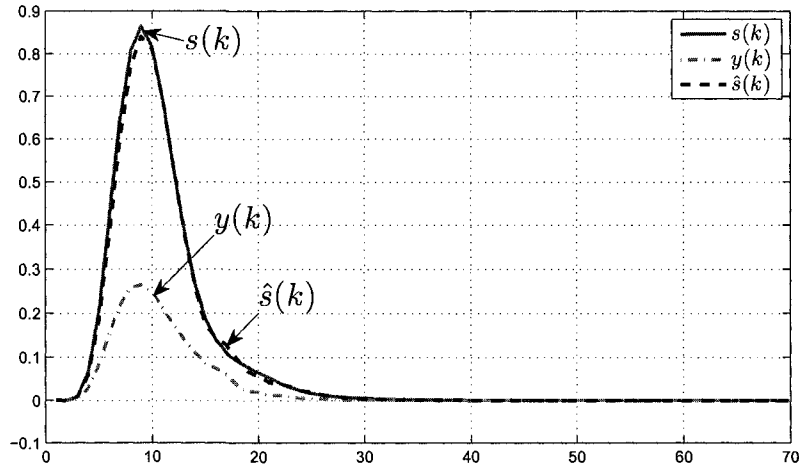
Figure 4.1: Example 2: Simulation results without channel noise.

Example 3: Then apply Corollary 4 to design the filter, and the results are:

$$
A_f = \begin{bmatrix}
8.0261 & -31.6036 & 34.6427 & -83.7086 & 59.1829 & -21.5709 & 188.4664 & -309.9510 & 132.2306 \\
2.5668 & -10.4777 & 12.0734 & -34.3011 & 24.0047 & -8.7353 & 80.5576 & -131.3303 & 55.5102 \\
0.8541 & -4.3466 & 7.8127 & -15.9327 & 10.5072 & -3.5367 & 27.6699 & -44.8258 & 18.8268 \\
0.1797 & -1.2453 & 2.9976 & -4.2525 & 3.0496 & -1.0362 & 5.8688 & -9.7621 & 4.1957 \\
-0.2069 & 1.0328 & -2.1393 & 3.1987 & -1.0323 & 0.2354 & -1.0217 & 1.1507 & -0.3114 \\
-0.3541 & 1.9554 & -4.3034 & 5.4613 & -2.4126 & 1.0108 & -2.2753 & 3.2028 & -1.2151 \\
-0.2708 & 1.6502 & -4.1543 & 5.4964 & -3.7329 & 1.2154 & 0.4467 & 0.3345 & -0.1881 \\
-0.3642 & 2.1427 & -5.0688 & 7.0390 & -4.9053 & 1.6289 & -1.8177 & 3.9125 & -1.5083 \\
-0.3451 & 2.0785 & -4.9285 & 7.1272 & -5.1267 & 1.7404 & -2.8284 & 5.0529 & -1.6158
\end{bmatrix},
$$

$$
B_f = \begin{bmatrix} 1273 & 560.29 & 199.53 & 48.672 & 1.3909 & -7.401 & 2.7556 & -8.8483 & -12.722 \end{bmatrix}^{\mathrm{T}},
$$

45
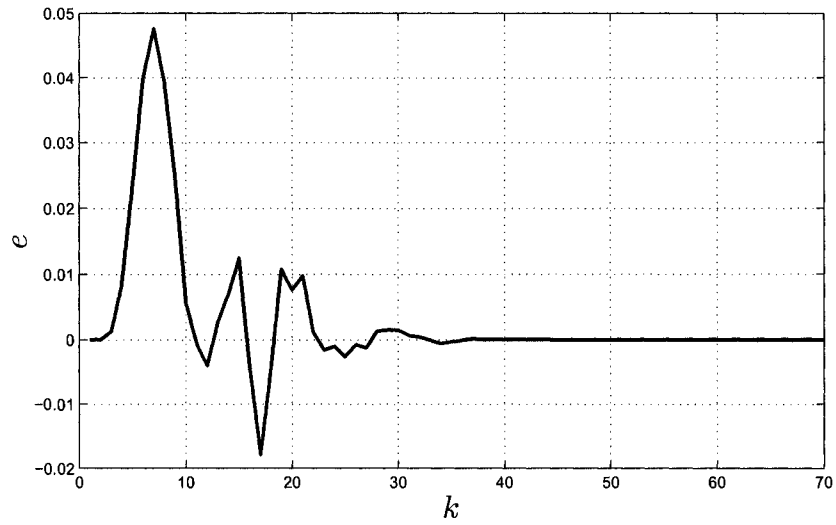
Figure 4.2: Example 2: Reconstructed error signal without channel noise.
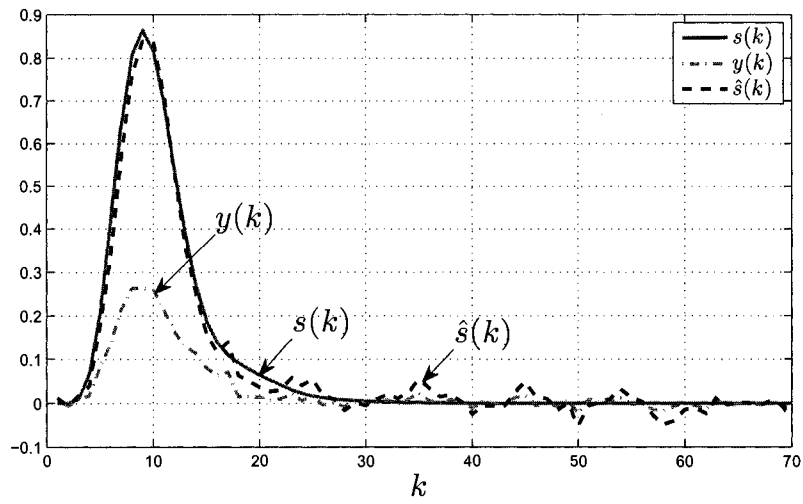
Figure 4.3: Example 2: Simulation results with channel noise.

$$C_f = \begin{bmatrix} -0.011639 & 0.044552 & -0.065991 & 0.056478 & 0.0079402 & -0.0098903 & 0.13346 & -0.25943 & 0.1239 \end{bmatrix},$$

$$D_f = 2.001.$$

46
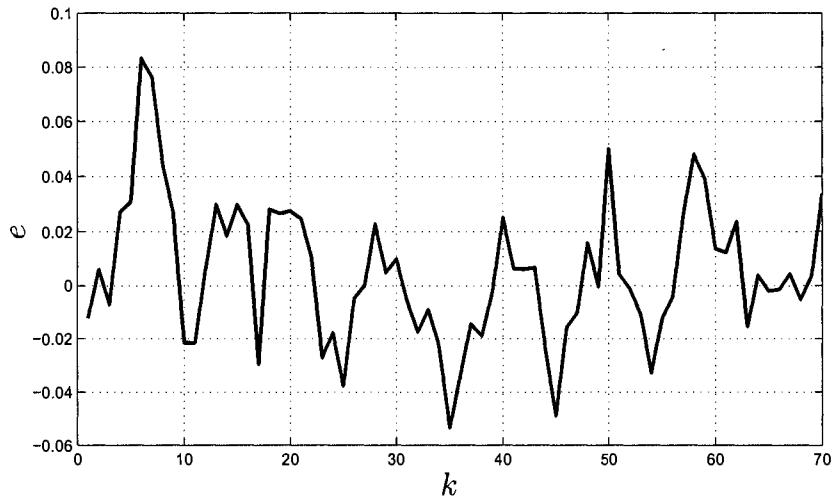
Figure 4.4: Example 2: Reconstructed error signal with channel noise.

Figure 4.5 shows the filter output $\hat{s}(k)$, signals $s(k)$ and $y(k)$ without channel noise $v(k)$. The signal reconstruction error is shown in Figure 4.6. Then, a white noise with power of 1×10^{-4} is added and the results are shown in Figures 4.7 and 4.8.
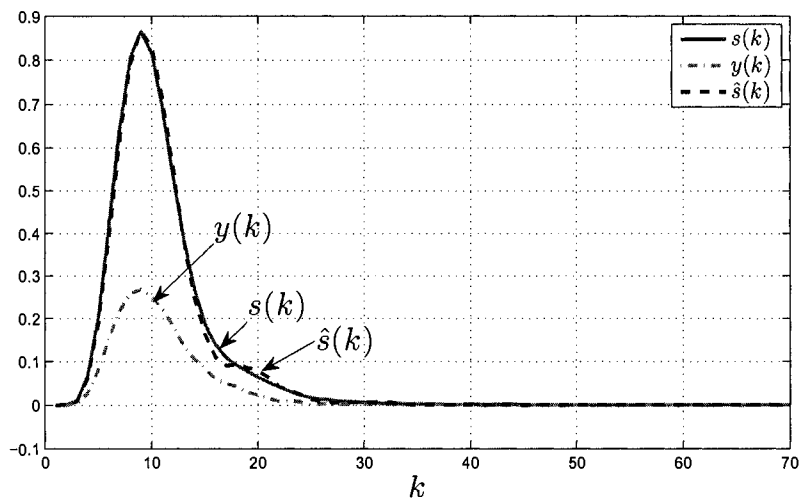
Figure 4.5: Example 3: Simulation results without channel noise.
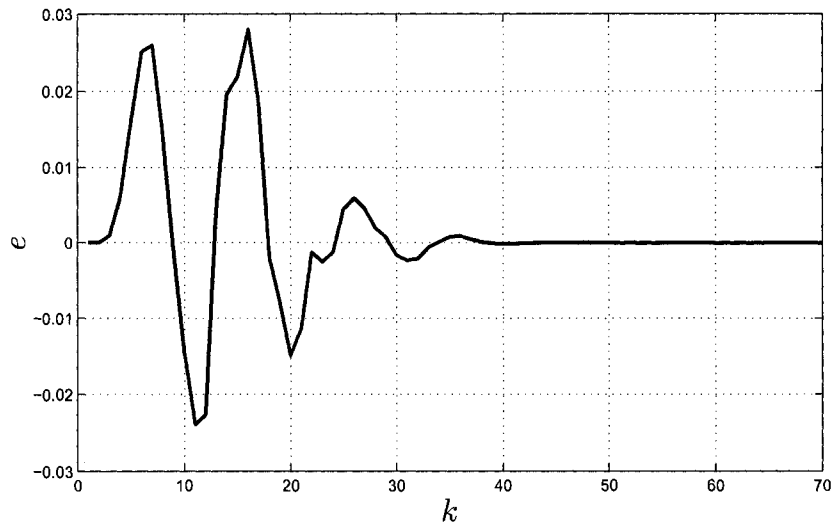
Figure 4.6: Example 3: Signal reconstruction error without channel noise.
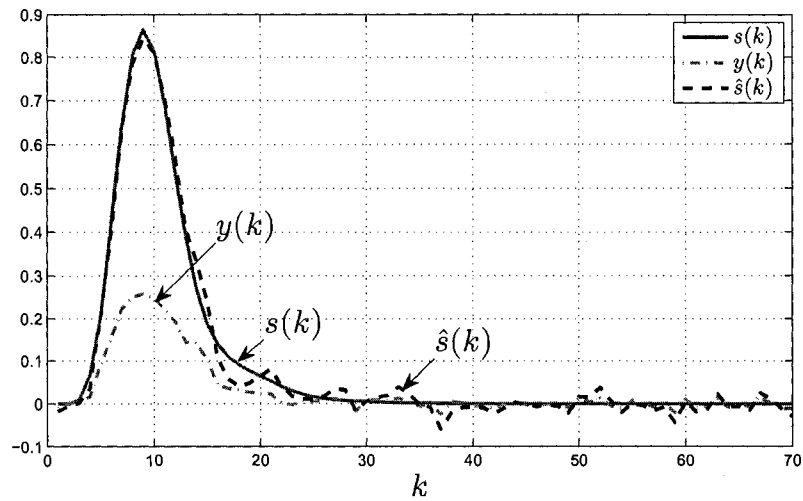
Figure 4.7: Example 3: Simulation results with channel noise.

The comparisons of signal reconstruction errors are shown in Figures 4.9 and 4.10, respectively.

From Table 4.1 and all the simulation figures, it is obvious that the parameter-
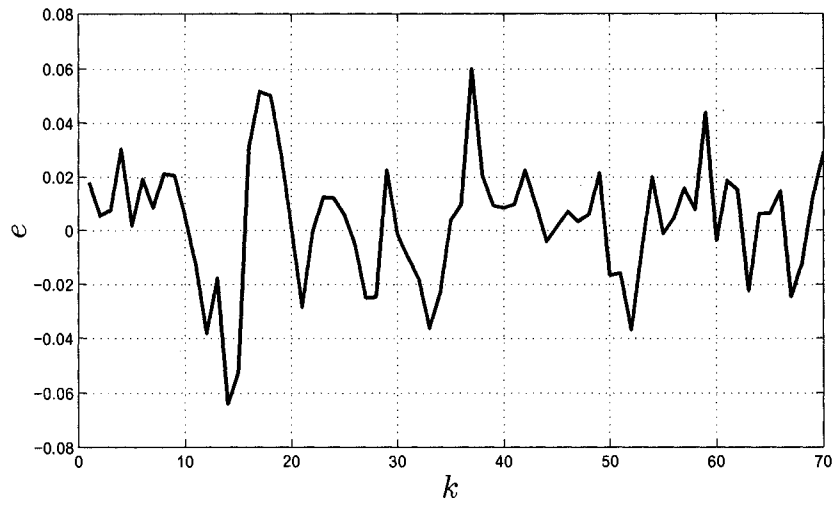
Figure 4.8: Example 3: Signal reconstruction error without channel noise.
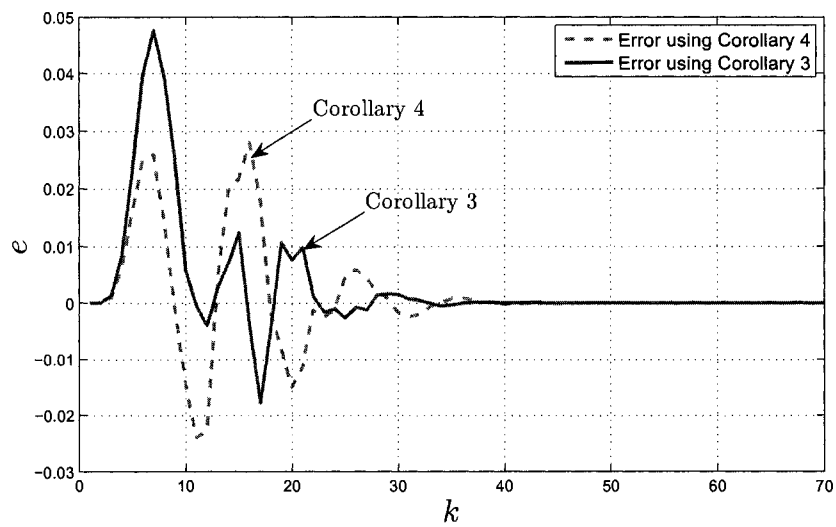
Figure 4.9: Comparison of error signals without noise.

dependent Lyapunov method achieves much less conservative design that the direct method.
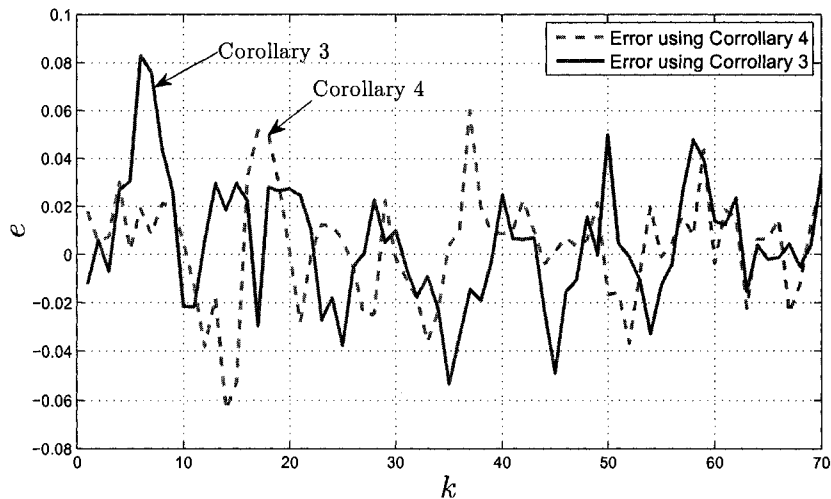
Figure 4.10: Comparison of error signals with noise.

4.5 Conclusion

In this chapter, first, by directly extending the results of Chapter 3, we develop the robust $l_2 - l_\infty$ IIR deconvolution filter incorporating the polytopic channel uncertainties; this direct extension is enabled by the inherent properties of convex combination for this type of uncertainty description. However, such a straightforward extension leads to conservativeness to some extent. Therefore, we apply the so called parameter-dependent Lyapunov method to re-design the robust $l_2 - l_\infty$ deconvolution filter, resulting in less conservativeness in terms of the smaller $l_2 - l_\infty$ gain, and for sure, better signal reconstruction performance. Several examples are given to verify the proposed methods.

Chapter 5

Conclusions and Future Work

In this thesis, we have investigated the deconvolution filter design with guaranteed energy-to-peak performance, that is, the $l_2 - l_\infty$ deconvolution filter design. This chapter summarizes the results reported in this thesis, and proposes some possible future research directions.

5.1 Conclusions

Unlike most existing deconvolution filtering design methods under the framework of $\mathcal{H}_\infty$ optimization in the literature, we propose to design $l_2 - l_\infty$ deconvolution filters.

1. We have proposed to design FIR deconvolution filters that guarantee the energy-to-peak performance using the LMI-based optimization approach and the PRA method. Simulation studies show that for FIR filters, the longer the filter length, the better performance can be achieved.

2. We have developed the $l_2 - l_\infty$ IIR deconvolution filter by using the LMI technique. The IIR filter is found to outperform the FIR one. One way to improve the performance of FIR deconvolution filters is to increase the filter length.

3. By directly extending the results of $l_2 - l_\infty$ deconvolution filter design in Chapter 3, we have developed the robust $l_2 - l_\infty$ IIR deconvolution filter incorporating the polytopic channel uncertainties; this direct extension is enabled by the inherent properties of convex combination for this type of uncertainty description. However, such a straightforward extension leads to conservativeness to some extent. Therefore, we have further applied the parameter-dependent Lyapunov method to re-design the robust $l_2 - l_\infty$ deconvolution filter, result-

ing in less conservativeness in terms of the smaller $l_2 - l_\infty$ gain, and for sure, better signal reconstruction performance.

In the following section, we give some possible future research directions.

5.2   Future Work

Indeed, even though present analysis and design of deconvolution filters go a long way in facilitating reliable applications, in many aspects the research in this area is still open. We propose some future research topics.

- Existing deconvolution filter design methods are based on infinite precision arithmetic, and therefore lead to filters that cannot be readily implemented with microprocessors. Such infinite precision filters have to be transformed into finite precision filters using techniques such as coefficient quantization and rounding before they can be implemented with hardware. This leads to two problems: (1) First, the likely sacrifice of filter performance because of the deviation from the infinite precision filter (which can be partially overcome by increasing the level of precision, although practical applications have a limit to the allowed wordlength); (2) second, the use of more bits tends to exacerbate the cost and complexity of hardware implementation. Hence, it is interesting to design deconvolution filters whose coefficients are restricted to a sum of signed powers of two (POT). This feature allows the filters to be implemented with simple adders and shifters only, eliminating the need to use any multipliers whose contribution to the cost and complexity is often great. This type of deconvolution filters is desirable in applications. The design could be formulated as an integer programming problem under the framework of model matching.

- On another practical side, lower filter order and complexity are always required in many applications. It would be interesting to further study the design of deconvolution filters with designable filter length. To develop an efficient algorithm to simultaneously design both deconvolution filter parameters and filter length is the main objective.

- In practice, signal transmission is usually affected by the network-induced packet loss and/or delay, as depicted in Figure 5.1. Therefore, the output measurements $y\prime(k)$ will be subject to random data loss. An obvious consequence is that the deconvolution filter design will become more challenging: Since the output data are not always available, existing deconvolution filter design methods can no longer be applied directly. How to design an effective deconvolution filter with randomly missing outputs is a worthy topic for future research.
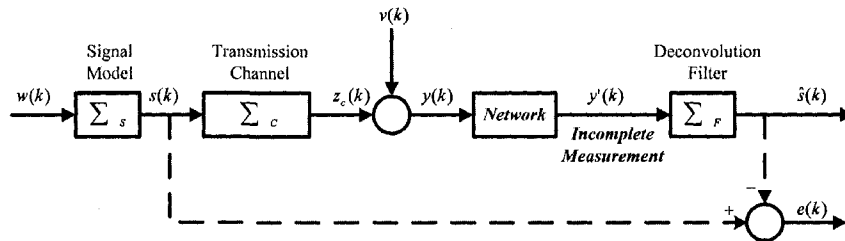
Figure 5.1: A deconvolution filtering system with randomly missing outputs.

Chapter 6

Appendix: Proof of Theorem 6

Proof: *Proof of necessity.* Suppose there exists an admissible filter guaranteeing the filtering error system to be stable with an $l_2 - l_\infty$ disturbance attenuation level γ, then from Theorem 4, there exist matrices $0 < Y$ and G satisfying (4.10) and (4.11). Partition G, G^{-1} and Y as

$$G = \begin{bmatrix} G_{11} & G_{12} \\ G_{21} & G_{22} \end{bmatrix} \quad G^{-1} = \begin{bmatrix} S_{11} & S_{12} \\ S_{21} & S_{22} \end{bmatrix} \quad Y = \begin{bmatrix} Y_{11} & Y_{12} \\ Y_{12}^{\mathrm{T}} & Y_{22} \end{bmatrix}. \tag{6.1}$$

There is no loss of generality in assuming that G_{21} and S_{21} are invertible. Introduce matrices

$$J_G := \begin{bmatrix} G_{11} & I \\ G_{21} & 0 \end{bmatrix} \quad J_S := \begin{bmatrix} I & S_{11} \\ 0 & S_{21} \end{bmatrix} \tag{6.2}$$

then J_G and J_S are nonsingular, and we have

$$G^{-1}J_G = J_s \quad GJ_S = J_G. \tag{6.3}$$

Define

$$\hat{Y} := \begin{bmatrix} \hat{Y}_{11} & \hat{Y}_{12} \\ \hat{Y}_{12}^{\mathrm{T}} & \hat{Y}_{22} \end{bmatrix}. \tag{6.4}$$

Performing congruence transformations to (4.10) by $J_5 := \mathrm{diag}\{I, J_S, I\}$, and to (4.11) by $J_6 := \mathrm{diag}\{J_S, J_S, I\}$, yields

$$\begin{bmatrix} \gamma^2 I & LG_{11} - C_f G_{21} & L & \Gamma - D_f D \\ * & G_{11}^{\mathrm{T}} + G_{11} - \hat{Y}_{11} & I + G_{11}^{\mathrm{T}} S_{11} + G_{21}^{\mathrm{T}} S_{21} - \hat{Y}_{12} & 0 \\ * & * & S_{11} + S_{11}^{\mathrm{T}} - \hat{Y}_{22} & 0 \\ * & * & * & I \end{bmatrix} > 0, \tag{6.5}$$

$$\begin{bmatrix} \hat{Y}_{11} & \hat{Y}_{12} & AG_{11} & A & B \\ * & \hat{Y}_{22} & S_{11}^{\mathrm{T}} AG_{11} + S_{21}^{\mathrm{T}} B_f C G_{11} + S_{21}^{\mathrm{T}} A_f G_{21} & S_{11}^{\mathrm{T}} A + S_{21}^{\mathrm{T}} B_f C & S_{11}^{\mathrm{T}} B + S_{21}^{\mathrm{T}} B_f D \\ * & * & G_{11} + G_{11}^{\mathrm{T}} - \hat{Y}_{11} & I + G_{11}^{\mathrm{T}} S_{11} + G_{21}^{\mathrm{T}} S_{21} - \hat{Y}_{12} & 0 \\ * & * & * & S_{11} + S_{11}^{\mathrm{T}} - \hat{Y}_{22} & 0 \\ * & * & * & * & I \end{bmatrix} > 0. \tag{6.6}$$

Inequality (6.5) implies $G_{11} + G_{11}^{\mathrm{T}} - \hat{Y}_{11} > 0$, then G_{11} is invertible. Performing congruence transformations to (6.5) by $J_7 := \mathrm{diag}\{I, G_{11}^{-1}, I\}$, and to (6.6) by $J_8 :=$

diag$\{G_{11}^{-1}, I, G_{11}^{-1}, I, I\}$ yields

$$\begin{bmatrix} \gamma^2 I & L - C_f G_{21} G_{11}^{-1} & L & \Gamma - D_f D \\ * & G_{11}^{-T} + G_{11}^{-1} - X & G_{11}^{-T} + S_{11} + G_{11}^{-T} G_{21}^T S_{21} - Z & 0 \\ * & * & S_{11} + S_{11}^T - V & 0 \\ * & * & * & I \end{bmatrix} > 0, \quad (6.7)$$

$$\begin{bmatrix} X & Z & G_{11}^{-T} A & G_{11}^{-T} A & G_{11}^{-T} B \\ * & V & S_{11}^T A + S_{21}^T B_f C + S_{21}^T A_f G_{21} G_{11}^{-1} & S_{11}^T A + S_{21}^T B_f C & S_{11}^T B + S_{21}^T B_f D \\ * & * & G_{11}^{-T} + G_{11}^{-1} - X & G_{11}^{-T} + S_{11} + G_{11}^{-T} G_{21}^T S_{21} - Z & 0 \\ * & * & * & S_{11} + S_{11}^T - V & 0 \\ * & * & * & * & I \end{bmatrix} > 0 \tag{6.8}$$

where

$$\bar{Y} := \begin{bmatrix} X & Z \\ Z^T & V \end{bmatrix} = \begin{bmatrix} G_{11}^{-1} & 0 \\ 0 & I \end{bmatrix} \begin{bmatrix} Y_{11} & Y_{12} \\ Y_{12}^T & Y_{22} \end{bmatrix} \begin{bmatrix} G_{11}^{-1} & 0 \\ 0 & I \end{bmatrix}$$

$$= \begin{bmatrix} G_{11}^{-T} & 0 \\ S_{11}^T & S_{21}^T \end{bmatrix} \begin{bmatrix} Y_{11} & Y_{12} \\ Y_{12}^T & Y_{22} \end{bmatrix} \begin{bmatrix} G_{11}^{-1} & S_{11} \\ 0 & S_{21} \end{bmatrix} \tag{6.9}$$

and a new change of variables to (6.7) and (6.8) defined by

$$R := G_{11}^{-1}, \ F := S_{11}, \ U := S_{21}^T G_{21} R,$$

$$M := S_{21}^T A_f G_{21} R, N := S_{21}^T B_f, \tag{6.10}$$

$$T := C_f G_{21} R$$

yields LMIs (4.14) and (4.15).

Proof of Sufficiency. Suppose there exist matrices $0 < X$, $0 < V$, Z, R, F, M, N, T, D_f satisfying (4.14) and (4.15), then the proof is as follows. LMI (4.15) implies

$$\begin{bmatrix} X & Z \\ * & V \end{bmatrix} > 0, \quad \begin{bmatrix} R^T + R - X & R^T + F + U^T - Z \\ * & F^T + F - V \end{bmatrix} > 0. \tag{6.11}$$

Further, we have

$$\begin{bmatrix} R^T + R & R^T + F + U^T \\ * & F^T + F \end{bmatrix} > 0. \tag{6.12}$$

Then, U must be nonsingular, or there exists $x \neq 0$ satisfying $Ux = 0$ which gives rise to

$$\begin{bmatrix} x^T & -x^T \end{bmatrix} \begin{bmatrix} R^T + R & R^T + F + U^T \\ * & F^T + F \end{bmatrix} \begin{bmatrix} x \\ -x \end{bmatrix} = 0 \tag{6.13}$$

57

which contradicts (6.12). With R nonsingular, invertible G_{21} and S_{21} can always be constructed from $UR^{-1} = S_{21}^{\mathrm{T}}G_{21}$. Then the filter matrices A_f, B_f, C_f as well as S_{11} and G_{11} can be constructed uniquely from (6.10). In addition, we can also compute Y_{11}, Y_{12}, and Y_{22} by reversing the formulas.

Since G_{21}, S_{21}, and S_{11} are invertible, the matrices J_G, J_S, J_1, J_2, J_3, and J_4 defined above are all invertible. By adequate transformations and congruence transformation, (4.14) and (4.15) are equivalent to (4.10) and (4.11). Then we can conclude that the filtering error system is stable with an $l_2 - l_\infty$ disturbance attenuation level γ.

Furthermore, from (6.10), we have

$$A_f = S_{21}^{\mathrm{T}}MR^{-1}G_{21}^{-1}, \quad B_f = S_{21}^{-\mathrm{T}}N, \quad C_f = TR^{-1}G_{21}^{-1}. \tag{6.14}$$

Then the transfer function (in z) of the filter is described by $T(z) = C_f(zI - A_f)^{-1}B_f$. The change of variables defined in (6.14) together with some standard transformations to the above transfer function yields

$$T(z) = T(zI - U^{-1}M)^{-1}U^{-1}N, \tag{6.15}$$

which means (4.16) is established and the proof is concluded. $\qquad\square$

Bibliography

[1] S. K. Alam, J. Ophir, I. Céspedes, and T. Varghese, "A deconvolution filter for improvement of time-delay estimation in elastography," *IEEE Transactions on Ultrasonics, Ferroelectrics, and Frequency Control*, vol. 45, no. 6, pp. 1565–1572, Nov. 1998.

[2] J. J. Anaya, L. G. Ullate, and C. Fritsch, "A method for real-time deconvolution," *IEEE Transactions on Instrumentation and Measurement*, vol. 41, no. 3, pp. 413–419, June 1992.

[3] R.G. Brown and P.Y.C. Hwang, *Introduction to Random Signals and Applied Kalman Filtering*, John Wiley and Sons, 19992.

[4] A. Chai and Z. Shen, "Deconvolution: a wavelet frame approach," *Numerische Mathematik*, vol. 106, no. 4, pp. 529–587, June 2007.

[5] B.-S. Chen, Y.-C. Chung, and D.-F. Huang, "Optimal time-frequency deconvolution filter design for nonstationary signal transmission through a fading channel: AF filter bank approach," *IEEE Transactions on Signal Processing*, vol. 46, no. 12, pp. 3220–3234, Dec. 1998.

[6] ——, "A wavelet time-scale deconvolution filter design for nonstationary signal transmission systems through a multipath fading channel," *IEEE Transactions on Signal Processing*, vol. 47, no. 5, pp. 1441–1446, May 1999.

[7] B.-S. Chen and W.-S. Hou, "Deconvolution filter design for fractal signal transmission systems: A multiscale kalman filter bank approach," *IEEE Transactions on Signal Processing*, vol. 45, no. 5, pp. 1359–1364, May 1997.

[8] B.-S. Chen and J.-C. Hung, "Fixed-order H_2 and H_∞ optimal deconvolution filter designs," *Signal Processing*, vol. 80, no. 2, pp. 311–331, Feb. 2000.

[9] Y.-L. Chen and B.-S. Chen, "Minimax robust deconvolution filters under stochastic parametric and noise uncertainties," *IEEE Transactions on Signal Processing*, vol. 42, no. 1, pp. 32–45, Jan. 1994.

[10] Y.-M. Cheng, B.-S. Chen, and L.-M. Chen, "Minimax deconvolution design of multirate systems with channel noises: A unified approach," *IEEE Transactions on Signal Processing*, vol. 47, no. 11, pp. 3145–3149, Nov. 1999.

[11] M. Corless, G. Zhu, and R. Skelton, "Improved robustness bounds using covariance matrices," *Proceedings of the 28th Conference on Decision and Control*, Tampa, Florida, December 1989.

[12] F. A. Cuzzola and A. Ferrante, "Explicit formulas for LMI-based H_2 filtering and deconvolution," *Automatica*, vol. 37, no. 9, pp. 1443–1449, Sept. 2001.

[13] M. de Oliveira, J. Bernussou, and J. Geromel, "A new discrete-time robust stability condition," *Systems and Control Letters*, vol. 37, no. 4, pp. 261–265, July 1999.

[14] F. DellAcqua, G. Rizzo, P. Scifo, R. A. Clarke, G. Scotti, , and F. Fazio, "A model-based deconvolution approach to solve fiber crossing in diffusion-weighted MR imaging," *IEEE Transactions on Biomedical Engineering*, vol. 54, no. 3, pp. 462–472, Mar. 2007.

[15] C. C. Enz and F. Krummenacher, "Continuous-time deconvolution filters for gas proportional detectors," *Electronics Letters*, vol. 29, no. 5, pp. 507–508, Mar. 1993.

[16] H. Gao and C. Wang, "Robust energy-to-peak filtering with improved LMI representations," *IEE Proceedings - Vision, Image, and Signal Processing*, vol. 150, no. 2, pp. 82–89, Apr. 2003.

[17] H. Gao, J. Lam, and C. Wang, "Mixed $\mathcal{H}_2/\mathcal{H}_\infty$ filtering for continuous-time polytopic systems: A parameter-dependent approach," *Circuits, Systems, and Signal Processing*, vol. 24, no. 6, pp. 689–702, 2005.

[18] K. M. Grigoriadis and J. T. Watson, "Reduced-order H_∞ and L_2-L_∞ filtering via linear matrix inequalities," *IEEE Transactions on Aerospace and Electronic Systems*, vol. 33, no. 4, pp. 1326–1338, Oct. 1997.

[19] T. C. Hanshaw, M. J. Anderson, and C. S. Hsu, "An H_∞ deconvolution filter and its application to ultrasonic nondestructive evaluation of materials," in *Proceedings of the American Control Conference*, San Diego, California, June 1999, pp. 3878–3884.

[20] B. Hassibi, A. H. Sayed, and T. Kailath, Indefinite-Quadratic Estimation and Control A Unified Approach to $\mathcal{H}_2$ and $\mathcal{H}_\infty$ Theories. Prentice-Hall, Englewood. Cliffs, N.J, 1999.

[21] J.-C. Hung and B.-S. Chen, "Genetic algorithm approach to fixed-order mixed H_2/H_∞ optimal deconvolution filter designs," *IEEE Transactions on Signal Processing*, vol. 48, no. 12, pp. 3451–3461, Dec. 2000.

[22] Y. Inouye and K. Tanebe, "Super-exponential algorithms for multichannel blind deconvolution," *IEEE Transactions on Signal Processing*, vol. 48, no. 3, pp. 881–888, Mar. 2000.

[23] J.-Y. Koo and P. T. Kim, "Asymptotic minimax bounds for stochastic deconvolution over groups," *IEEE Transactions on Information Theory*, vol. 54, no. 1, pp. 289–298, Jan. 2008.

[24] L. D. Lathauwer and A. de Baynast, "Blind deconvolution of DS-CDMA signals by means of decomposition in rank-$(1, L, L)$ terms," *IEEE Transactions on Signal Processing*, vol. 56, no. 4, pp. 1562–1571, Apr. 2008.

[25] C.-M. Lee and I.-K. Fong, "Robust FIR filter design with envelope constraints and channel uncertainty," *IEEE Transactions on Signal Processing*, vol. 52, no. 6, pp. 1797–1801, June 2004.

[26] H. Lee and B. Noorbehesht, "Optimal deconvolution filter for high-resolution NMR spectral parameter estimation," *Acoustics, Speech, and Signal Processing*, vol. 2, pp. 1316–1319, Apr. 1988.

[27] H. Li and M. Fu, "A linear matrix inequality approach to robust H_∞ filtering," *IEEE Transactions on Signal Processing*, vol. 45, no. 9, pp. 2338–2350, Sept. 1997.

[28] X. Lu, H. Zhang, W. Wang, and C. Zhang, "A new approach to H_∞ deconvolution filtering," in *Proceedings of the American Control Conference*, Minneapolis, Minnesota, USA, June 2006, pp. 5644–5649.

[29] C. T. Ma, Z. Ding, and S. F. Yau, "A two-stage algorithm for MIMO blind deconvolution of nonstationary colored signals," *IEEE Transactions on Signal Processing*, vol. 48, no. 4, pp. 1187–1192, Apr. 2000.

[30] R. Neelamani, H. Choi, and R. Baraniuk, "ForWaRD: Fourier-wavelet regularized deconvolution for ill-conditioned systems," *IEEE Transactions on Signal Processing*, vol. 52, no. 2, pp. 418–433, Feb. 2004.

[31] R. Neelamani, M. Deffenbaugh, and R. G. Baraniuk, "Texas two-step: A framework for optimal multi-input single-output deconvolution," *IEEE Transactions on Image Processing*, vol. 16, no. 11, pp. 2752–2765, Nov. 2007.

[32] M. C. de Oliveira, J. Bernussou and J. C. Geromel, "A new discrete-time robust stability condition," *System & Control Letters*, vol. 37, no. 2, pp. 261–265, 1997.

[33] M. C. de Oliveira and J. C. Geromel, "Numerical comparison of output feedback design methods," in *Proc. Amer. Control Conf.*, vol. 1, Albuquerque, NM, USA, June 1997, pp. 72–76.

[34] R. M. Palhares and P. L. Peres, "Robust filtering with guaranteed energy-to-peak performance – an LMI approach," *Automatica*, vol. 36, no. 6, pp. 851–858, June 2000.

[35] N. G. Paulter, "A causal regularizing deconvolution filter for optimal waveform reconstruction," *IEEE Transactions on Instrumentation and Measurement*, vol. 43, no. 5, pp. 740–747, Oct. 1994.

[36] S.-C. Peng and B.-S. Chen, "Deconvolution filter design via l_1 optimization technique," *IEEE Transactions on Signal Processing*, vol. 45, no. 3, pp. 736–746, Mar. 1997.

[37] D.-T. Pham, "Generalized mutual information approach to multichannel blind deconvolution," *Signal Processing*, vol. 87, no. 9, pp. 2045–2060, Sept. 2007.

[38] G. Pillonetto and B. M. Bell, "Bayes and empirical bayes semi-blind deconvolution using eigenfunctions of a prior covariance," *Automatica*, vol. 43, no. 10, pp. 1698–1712, Oct. 2007.

[39] K. P. Prasad and R. Unbehauen, "A different recursive formulation of 2-D digital inverse filter," *Circuits and Systems*, vol. 1, pp. 587–590, May 1993.

[40] R. Rajagopal and L. C. Potter, "Multivariate MIMO FIR inverses," *IEEE Transactions on Image Processing*, vol. 12, no. 4, pp. 458–465, Apr. 2003.

[41] H. Rho and C. S. Hsu, "A game theory appooach to H_∞ deconvolution filter design," in *Proceedings of the American Control Conference*, San Diego, California, June 1999, pp. 2891–2895.

[42] ——, "A reduced order H_∞ deconvolution filter design using bounded real lemma," in *Proceedings of the American Control Conference*, Arlington, VA, June 2001, pp. 4234–4240.

[43] H. Rho, C. S. Hsu, and H. Kim, "A reduced-order H_∞ deconvolution filter design using bounded real lemma," *Signal Processing*, vol. 86, no. 7, pp. 1688–1703, July 2006.

[44] M.A. Rotea, "The generalized H_2 control problem," *Automatica*, vol. 29, no. 2, pp. 373–385, 1993.

[45] I. Santamaría, C. J. Pantaleón, J. Ibánez, and A. Artés, "Deconvolution of seismic data using adaptive gaussian mixtures," *IEEE Transactions on Geoscience and Remote Sensing*, vol. 37, no. 2, pp. 855–859, Mar. 1999.

[46] T.-J. Su and C.-P. Wei, "An FIR equalizer design for nonlinear channels using hybrid GA and LMI," *Circuits, Systems, and Signal Processing*, vol. 25, no. 6, pp. 685–699, 2006.

[47] S.-L. Sun, "Distributed optimal component fusion deconvolution filtering," *Signal Processing*, vol. 87, no. 1, pp. 202–209, Jan. 2007.

[48] Z. Tan, Y. C. Soh, and L. Xie, "Envelope-constrained H_∞ FIR filter design," *IEEE Transactions on Circuits and Systems—Part II: Analog and Digital Signal Processing*, vol. 47, no. 1, pp. 79–82, Jan. 2000.

[49] ——, "Envelope-constrained H_∞ FIR filter design: an LMI optimization approach," *IEEE Transactions on Signal Processing*, vol. 48, no. 10, pp. 2960–2963, October 2000.

[50] ——, "Envelope-constrained H_2 FIR filter design," *Circuits, Systems, and Signal Processing*, vol. 18, no. 6, pp. 539–551, 1999.

[51] A. M. Tekalp and G. Pavlović, "Image restoration with multiplicative noise: Incorporating the sensor nonlinearity," *IEEE Transactions on Signal Processing*, vol. 39, no. 9, pp. 2132–2136, Sept. 1991.

[52] A. C. Tsoi and L. Ma, "A balanced approach to multichannel blind deconvolution," *IEEE Transactions on Circuits and Systems—Part I: Fundamental Theory and Applications*, vol. 55, no. 2, pp. 599–613, Mar. 2008.

[53] B. M. Tsui, H.-B. Hu, D. R. Gilland, and G. T. Gullberg, "Implementation of simultaneous attenuation and detector response correction in spect," *IEEE Transactions on Nuclear Science*, vol. 35, no. 1, pp. 778–783, Feb. 1988.

[54] T. E. Tuncer and M. Aktas, "LSE and MSE optimum partition-based FIR-IIR deconvolution filters with best delay," *IEEE Transactions on Signal Processing*, vol. 53, no. 10, pp. 3780–3790, Oct. 2005.

[55] G. Wei, Z. Wang, H. Shu, and J. Fang, "H_∞ deconvolution filters for stochastic systems with interval uncertainties," *Circuits, Systems, and Signal Processing*, vol. 26, no. 4, pp. 495–512, 2007.

[56] D.A. Wilson, "Convolution and Hankel operator norms for linear systems," *IEEE Transactions on Automatic Control*, vol. 34, no. 1, pp. 94–97, January 1989.

[57] L. Xie, C. Du, C. Zhang, and Y. C. Soh, "H_∞ deconvolution filtering of 2-d digital systems," *IEEE Transactions on Signal Processing*, vol. 50, no. 9, pp. 2319–2332, Sept. 2002.

[58] L. Xie, S. Wang, C. Du, and C. Zhang, "H_∞ deconvolution of periodic channels," *Signal Processing*, vol. 80, no. 11, pp. 2365–2378, Nov. 2000.

[59] S. Xu, J. Lam, H. Gao, and Y. Zou, "Robust H_∞ filtering for uncertain discrete stochastic systems with time delays," *Circuits, Systems, and Signal Processing*, vol. 24, no. 6, pp. 753–770, 2005.

[60] X. Yu, C. S. Hsu, and R. H. Bamberger, "H_∞ deconvolution filter design and its application in image restoration," in *Proceedings of the Conference on Decision and Control*, Kobe, Japan, Dec. 1996, pp. 4802–4807.

[61] Z. Zang, A. Cantoni, and K. L. Teo, "Envelope-constrained IIR filter design via $\mathcal{H}_\infty$ optimization methods," *IEEE Transactions on Circuits and Systems— Part I: Fundamental Theory and Applications*, vol. 46, no. 6, pp. 649–653, June 1999.

[62] H. Zhang, L. Xie, and Y. C. Soh, "H_∞ deconvolution filtering, prediction, and smoothing: A krein space poloynominal approach," *IEEE Transactions on Signal Processing*, vol. 48, no. 3, pp. 888–892, Mar. 2000.

[63] L. Zhang, B. Huang, and J. Lam, "H_∞ model reduction of markovian jump linear systems," *Syst. Control Lett.*, vol. 50, no. 2, pp. 103–118, Oct. 2003.

[64] L. Zhang, A. Cichocki, and S. ichi Amari, "Multichannel blind deconvolution of nonminimum-phase systems using filter decomposition," *IEEE Transactions on Signal Processing*, vol. 52, no. 5, pp. 1430–1442, May 2004.

[65] Y. Zhang and J. Chambers, "Variable tap-length natural gradient blind deconvolution-equalisation algorithm," *Electronics Letters*, vol. 43, July 2007.

[66] H. Zhou, L. Xie, and C. Zhang, "A direct approach to H_2 optimal deconvolution of periodic digital channels," *IEEE Transactions on Signal Processing*, vol. 50, no. 7, pp. 1685–1698, July 2002.

[67] J. Zhou and M. N. Do, "Multidimensional multichannel FIR deconvolution using gröbner bases," *IEEE Transactions on Image Processing*, vol. 15, no. 10, pp. 2998–3007, Oct. 2006.